

UNCLASSIFIED ~~CONFIDENTIAL~~

Copy 5
RM H57H12

C2

NACA RM H57H12

NACA

RESEARCH MEMORANDUM

EFFECTS OF WING-MOUNTED EXTERNAL STORES
ON THE LONGITUDINAL AND LATERAL HANDLING QUALITIES OF
THE DOUGLAS D-558-II RESEARCH AIRPLANE

By Jack Fischel, Robert W. Darville, and Donald Reisert

High-Speed Flight Station
CLASSIFICATION CHANGED ~~SECRET~~ Edwards, Calif.

UNCLASSIFIED

To

By authority of *NACA TPA 9 Effective* Date *9-1-57*

NB 11-20-59

CLASSIFIED DOCUMENT

This material contains information affecting the National Defense of the United States within the meaning of the espionage laws, Title 18, U.S.C., Sec. 793 and 794, the transmission or revelation of which in any manner to an unauthorized person is prohibited by law.

NATIONAL ADVISORY COMMITTEE FOR AERONAUTICS

WASHINGTON
October 28, 1957

LIBRARY COPY

OCT 29 1957
LANGLEY AERONAUTICAL LABORATORY
LIBRARY, NACA
LANGLEY FIELD, VIRGINIA

~~CONFIDENTIAL~~

UNCLASSIFIED

NATIONAL ADVISORY COMMITTEE FOR AERONAUTICS

RESEARCH MEMORANDUM

EFFECTS OF WING-MOUNTED EXTERNAL STORES
ON THE LONGITUDINAL AND LATERAL HANDLING QUALITIES OF
THE DOUGLAS D-558-II RESEARCH AIRPLANE

By Jack Fischel, Robert W. Darville, and Donald Reisert

SUMMARY

The subsonic and transonic handling qualities of the Douglas D-558-II research airplane were investigated with several configurations of mid-semispan external stores in the altitude region between 20,000 and 40,000 feet. The configurations tested consisted of an underslung pylon on each wing, pylons plus simulated DAC (Douglas Aircraft Co.) 1,000-pound bombs, and pylons plus DAC 150-gallon fuel tanks. Results of the tests were compared with comparable data obtained with the clean airplane.

The pylon and the pylon-bomb configurations generally had a small or negligible effect on the handling qualities of the airplane. The trends exhibited in the characteristics measured with the pylon-tank configuration were generally the same as for the clean airplane; however, significant changes in the magnitude of the parameters measured were sometimes apparent, particularly at the higher speeds tested.

INTRODUCTION

Numerous wind-tunnel investigations have been performed to determine the effects of externally carried stores or packages (fuel tanks, bombs, rocket packs, etc.) on the characteristics of various high-performance aircraft (refs. 1 to 4). Little had been done, however, to determine in flight the effects of these external stores on the handling qualities, performance, and loads of a high-performance aircraft, and the aerodynamic loads on the stores. Therefore, the National Advisory Committee for Aeronautics has been conducting flight tests of the Douglas D-558-II research airplane with either a midsemispan underslung

~~CONFIDENTIAL~~

UNCLASSIFIED

pylon attached to each wing, the pylons plus simulated DAC (Douglas Aircraft Co.) 1,000-pound bombs, or the pylons plus DAC 150-gallon fuel tanks. For ease of reference these configurations will be referred to in this paper as the pylon configuration, small-store configuration, and large-store configuration, respectively. The effects of the stores on the subsonic and transonic longitudinal and lateral handling qualities of the airplane are presented and discussed in this paper. The results of the performance phase of the investigation are presented in reference 5.

This research was performed as part of the cooperative Air Force-Navy-NACA High-Speed Flight Program at the request of the Bureau of Aeronautics, Department of the Navy, and was conducted at the NACA High-Speed Flight Station at Edwards, Calif.

SYMBOLS

a_n	normal-load factor or acceleration, g units
a_t	transverse acceleration, g units
b	wing span, ft
C_{N_A}	airplane normal-force coefficient, $a_n W/qS$
$C_{N_{A\alpha}}$	rate of change of normal-force coefficient with angle of attack, $dC_{N_A}/d\alpha$, per deg
C_Y	lateral-force coefficient, $a_t W/qS$
$C_{Y\beta}$	rate of change of lateral-force coefficient with angle of sideslip, $dC_Y/d\beta$, per deg
c	wing chord, ft
F_a	aileron control force, lb
F_e	elevator control force, lb
$\frac{dF_e}{da_n}$	rate of change of elevator control force with normal acceleration, lb/g

F_r	rudder control force, lb
$\frac{dF_r}{d\beta}$	rate of change of rudder pedal force with sideslip angle, lb/deg
g	acceleration due to gravity, ft/sec ²
h_p	pressure altitude, ft
i_t	stabilizer setting with respect to fuselage center line, positive when leading edge of stabilizer is up, deg
M	free-stream Mach number
P	period of longitudinal or lateral oscillation with controls fixed, sec
p	rolling velocity, radians/sec
$pb/2V$	wing-tip helix angle, radians
$\frac{pb/2V}{\delta_a}$	variation of wing-tip helix angle with total aileron deflection, radians/deg
q	pitching velocity, radians/sec, or free-stream dynamic pressure, lb/sq ft
\dot{q}	pitching acceleration, radians/sec ²
r	yawing velocity, radians/sec
S	wing area, sq ft
$T_{1/2}$	time required for the longitudinal or lateral controls-fixed oscillation to damp to one-half amplitude, sec
t	time, sec
V	true airspeed, ft/sec
V_i	indicated airspeed, mph
W	airplane weight, lb

α	angle of attack of airplane center line, deg
β	angle of sideslip, deg
δ_a	total aileron deflection, deg
$\frac{d\delta_a}{d\beta}$	rate of change of aileron deflection with sideslip angle (apparent effective dihedral parameter)
δ_e	elevator deflection with respect to stabilizer, deg
$\frac{d\delta_e}{dC_{N_A}}$	rate of change of elevator deflection with airplane normal- force coefficient, deg
δ_r	rudder deflection with respect to vertical tail, deg
$\frac{d\delta_r}{d\beta}$	rate of change of rudder deflection with sideslip angle (apparent directional stability parameter)
δ_s	slat position, in.
ξ	damping ratio, $\sin \left[\tan^{-1} \left(\frac{0.111P}{T_{1/2}} \right) \right]$

Subscripts:

L	left
R	right

AIRPLANE AND STORES

The Douglas D-558-II airplane used in this investigation is equipped with both a rocket and a turbojet engine. The rocket engine, a Reaction Motors, Inc., LR8-RM-6, exhausts out the tail of the airplane, and a Westinghouse J34-WE-40 turbojet engine exhausts out the bottom of the fuselage between the wing and the tail. The airplane is air-launched from a Boeing B-29 mother airplane.

Figure 1 shows photographs of the airplane in both the large- and small-store configurations. Figure 2 presents a three-view drawing of the airplane in the large-store configuration. Pertinent dimensions and characteristics of the airplane are listed in table I.

The slats located along the leading edge and over the outer portion of the wing may be locked closed, or they may be unlocked and free floating. In the unlocked condition they are normally closed at low angles of attack or normal-force coefficient and open with increase in angle of attack. The left and right wing slats are interconnected and are always in approximately the same position relative to each other.

The airplane is equipped with an adjustable stabilizer for longitudinal trim, but no means were provided for trimming aileron and rudder-control forces. No aerodynamic balance or control-force boost system is used on any of the controls. Hydraulic dampers are installed on all control surfaces to aid in the prevention of control-surface "buzz." Dive brakes are located on the rear portion of the fuselage.

The pylon and the stores investigated were provided by the Douglas Aircraft Co. Though differing in size, the stores had similar shapes, and the tail fins were initially located in planes at 45° to the vertical. However, for ground clearance purposes, the fins on the large store were rotated 45° into the vertical and horizontal planes and the lower fin was removed. Since the pylons were designed for the large stores, it was necessary to modify them to fit the small stores. A drawing of each store configuration is presented in figure 3. Tables II to IV present the dimensions of the pylons, small stores, and large stores, respectively.

INSTRUMENTATION

Standard NACA recording instruments were installed in the airplane to measure the following quantities pertinent to this investigation:

- Airspeed
- Altitude
- Angle of attack
- Angle of sideslip
- Normal and transverse accelerations
- Roll, pitch, and yaw velocities
- Pitch acceleration

Elevator, stabilizer, aileron, rudder, and slat positions
Elevator, aileron, and rudder control forces

All instruments were synchronized by a common timer..

Airspeed, altitude, angle of attack, and angle of sideslip were measured on a fuselage nose boom. Angles of attack and sideslip are presented as measured, with only instrument corrections applied. The possible Mach number error is about ± 0.01 at $M < 0.80$ and increases to about ± 0.02 at $M \approx 0.95$.

TESTS

Static longitudinal stability and control characteristics were obtained from speed runs near 35,000 feet and wind-up turns between Mach numbers of 0.50 and 1.03 at altitudes between 22,200 feet and 39,400 feet. Usually, the higher Mach number turns were performed at higher altitudes. Elevator pulses, performed between Mach numbers of 0.49 and 0.75 at altitudes of 22,000 feet to 27,000 feet, were used to obtain the longitudinal dynamic characteristics. Low-speed data were obtained from 1 g stall approaches in the following conditions: slats locked; slats unlocked (free to float); and landing (slats unlocked, gear down, flaps down).

Static lateral and directional characteristics were obtained from gradually increasing constant flight-path sideslips, abrupt aileron rolls, and trim runs at Mach numbers between 0.44 and 1.04 at altitudes between 22,000 feet and 36,000 feet. Lateral damping characteristics were obtained from rudder pulses performed between Mach numbers of 0.50 and 0.87 and between altitudes of 20,000 feet and 32,000 feet.

Both the longitudinal and lateral pulses were abrupt inputs with an effort being made to return and hold the controls at the trim condition while the oscillation damped out.

The center of gravity for these tests was located between 24.0 and 27.4 percent of the mean aerodynamic chord for all configurations; this is similar to the center-of-gravity location at which the clean airplane was previously tested, thereby permitting a direct comparison of results.

RESULTS AND DISCUSSION

The results presented herein are somewhat limited - particularly in regard to the dynamic characteristics of the airplane - because only a few flights were obtained with each external-store configuration. Sufficient data were obtained, however, to establish trends of the effects of the stores on the stability and control characteristics of the airplane at subsonic and transonic speeds. Since most of the tests were performed in the large-store configuration and only small differences were noted in the data for the various configurations, most of the data presented are for the large-store configuration.

The incremental lift and drag effects for the large-store configuration are shown in reference 5 and indicate the appreciable increment of drag produced by the stores, especially at $M > 0.9$. In addition, the pilots commented that they detected an increased penalty in airplane performance with an increase in size of the stores investigated, particularly at transonic speeds.

Longitudinal Stability and Control Characteristics

Longitudinal trim.- The longitudinal trim characteristics of the D-558-II airplane in 1 g flight at an altitude of 35,000 feet in the configurations tested were stable to $M \approx 0.83$ (fig. 4). Above $M \approx 0.83$, the elevator required for trim exhibited several successively unstable and stable trends to $M \approx 0.98$; above this speed the airplane became extremely stable. Except for a difference in level of δ_e for trim, the trends for the airplane with the various store configurations were the same as for the clean airplane (ref. 6). Some of this difference in the level of δ_e required may be due to the stabilizer setting i_t ; however, lower values of trim control may be noted for the pylon and large-store configurations.

Dynamic characteristics.- The dynamic longitudinal characteristics of the airplane with stores are presented in figure 5. These data indicated a negligible effect of the pylon and small-store configurations on the period and damping characteristics of the clean airplane (ref. 7). The large-store configuration decreased the static stability, as evidenced by an increase in the period of about 0.7 second. Simultaneously, the damping ratio increased as much as 0.07. These effects for the large-store configuration resulted in a negligible effect on the time to damp to half amplitude. Pylon and small-store configurations also improved the damping ratio, but this improvement was less than with the

large-store configuration. The pilots could detect little or no effect of the stores on the dynamic characteristics of the airplane.

Accelerated maneuvers.— Time histories of several representative turns are presented in figure 6 for Mach numbers of 0.60, 0.80, and 0.95. Because only small differences were noted in the data for the different store configurations, only data for the large stores are presented. Stability plots for these turns are presented in figure 7. In most cases these maneuvers were not extended much beyond heavy buffet or a decrease in stability. After the airplane experienced the decrease in stability, a subsequent pitch-up followed at all speeds from $M \approx 0.5$ to 0.95; this was particularly severe at the lower altitudes and between Mach numbers of 0.80 and 0.95. The pilot reported that for moderate rate inputs, buffet provided ample warning to enable the pilot to remain below the pitch-up boundary. These effects were also exhibited by the clean airplane (ref. 6). In order to present control-position data for static trimmed conditions and to determine more accurately the angle of attack where the decrease in stability occurred, values of δ_e were corrected for pitching acceleration when necessary; these values are presented in figure 7. The angle of attack where the decrease in stability occurred is indicated by the vertical ticks adjacent to the curves of δ_e plotted against α in figure 7.

Comparisons of the variation of normal-force coefficient C_{N_A} and elevator deflection δ_e with angle of attack for the three store configurations are made for several Mach numbers in figure 8. The data for the clean airplane (ref. 6) are also presented. At small angles of attack the data for the three store configurations and the clean airplane are essentially the same in trend. Differences noted in the level of elevator position are a result of the different stabilizer settings used for these maneuvers. The decrease in stability noted previously for the large-store configuration during dynamic maneuvers (by the increased period of oscillation) was not apparent during the accelerated maneuvers performed. However, this decrease in stability did become apparent when a comparison was made of the values of the apparent stability parameter $d\delta_e/dC_{N_A}$ for the various configurations and the clean airplane, as will be discussed. At higher angles of attack the differences in the variations of δ_e with α result from the effects of the stores on airplane stability and may be the result of changes in the flow over the airplane empennage. The appreciable differences noted in the variation of δ_e with α for the various store configurations from $M = 0.95$ to $M = 1.00$ and angles of attack lower than 4° (fig. 8(c)) were probably due to the large differences in control effectiveness at each Mach number tested rather than to any effects of

the different store configurations. Above an angle of attack of 4° in the region from $M \approx 0.95$ to $M \approx 1.0$, the speed decreased rapidly during the maneuvers; therefore, the variations of δ_e with α exhibited by the various store configurations result from trim changes as well as changes in stability due to the stores. No apparent change in longitudinal control effectiveness was noticed by the pilots with the various configurations, other than the increase of mass inertia moments with the stores in attempting a wind-up turn.

Figure 9 presents the boundary for decreased stability for the three store configurations and the clean airplane (ref. 6). The boundaries for the store configurations were found to be essentially the same as for the clean airplane.

Values of the stability and control effectiveness parameters $C_{N_{A\alpha}}$, $d\delta_e/dC_{N_A}$, and dF_e/da_n for a Mach number range from 0.49 to 1.03 for the various store configurations are compared with comparable data for the clean airplane (ref. 6) in figure 10. The values of $C_{N_{A\alpha}}$ were essentially the same for the three store configurations and the clean airplane except between $M \approx 0.85$ and $M \approx 0.96$. In this region $C_{N_{A\alpha}}$ for the large-store configuration decreased rapidly to a value of 0.074 at $M = 0.91$, then increased with increase in Mach number to $M \approx 0.96$. From the limited data obtained with the small-store configuration, it could not be determined if $C_{N_{A\alpha}}$ for this configuration had the same decrease between $M = 0.85$ and 0.96 as noted in the large-store data.

For all configurations tested, the apparent stability parameter $d\delta_e/dC_{N_A}$ was approximately constant at a value of about 9 below $M = 0.80$ and increased rapidly to about 60 at $M = 1.02$. Although slightly lower in value, the trends of $d\delta_e/dC_{N_A}$ with Mach number for the store configurations were the same as for the clean airplane.

The stick-force gradient dF_e/da_n increased gradually from a constant value of about 10 lb/g below $M = 0.75$ to a value of about 22 lb/g at $M = 0.90$. Above $M = 0.90$, values of dF_e/da_n increased rapidly to a value of over 120 lb/g at $M \approx 1.02$. The stores decreased slightly the values of dF_e/da_n over the speed range tested, but the basic trends of the data for the store configurations and the clean airplane were the same.

Buffet boundary.- Figure 11 compares the buffet boundary for the three store configurations with the boundary for the clean airplane (ref. 6). The pylon and small-store configurations have essentially the same boundary as the clean configuration. However, the buffet boundary was generally lower for the large-store configuration and was readily apparent to the pilot. Pilots reported that the intensity of buffeting encountered above the buffet boundary generally appeared heavier with the store configurations (especially with the large store) than with the clean airplane.

Low-Speed Characteristics

Stall approaches were performed with the airplane in each of the three store configurations. However, since no appreciable difference was found due to configuration, time histories (fig. 12) and stability plots (fig. 13) are presented only for the large-store configuration. The stall approach conditions tested were slats locked (figs. 12(a) and 13(a)), slats unlocked and free to float (figs. 12(b) and 13(b)), and the landing configuration (figs. 12(c) and 13(c)).

The data of figures 12 and 13 show that the stability of the airplane increased and was maintained to a lower speed when the slats were unlocked; stability was further improved in the landing condition. It will be noted that in the slats-unlocked condition, the pilot maintained the stall-approach maneuver to a lower speed than in the landing condition; however, appreciable longitudinal and lateral unsteadiness are apparent at these lower speeds. In general, with a decrease in speed all stall-approach maneuvers were accompanied by increased lateral and longitudinal unsteadiness, which was also characteristic of the clean airplane (ref. 8).

A comparison of the variations of airplane normal-force coefficient and elevator deflection with angle of attack for each of the store configurations is presented in figure 14. The stores appeared to have little, if any, effect on the normal-force-curve slope when compared to the basic airplane data (ref. 8). These data for the basic airplane are not included in this paper because they are essentially the same as the data for the store configurations. Except for a slightly different level of δ_e for a given angle of attack (attributed to different stabilizer settings), the trends indicated by the variation of δ_e with α for the different store configurations and the basic airplane were the same. All configurations had a neutral or negative stability at the higher angles of attack.

With the large-store configuration the pilots reported that the low-speed characteristics in smooth air during a landing pattern were essentially the same as for the clean airplane. In rough air, however, the airplane responded less to initial gusts with the store attached, and less control was necessary during an approach to a landing. If the airplane began rolling and yawing upon encountering rough air, damping with the large-store configuration was less than with the clean airplane and a tendency to overcontrol or even cross-control was apparent. No appreciable change in airplane attitude was noticed during touchdown with any configuration.

Lateral Stability and Control Characteristics

Lateral and directional trim.- The lateral and directional trim characteristics of the airplane with stores are compared with the data for the clean airplane (previously unpublished) in figure 15. Generally, the rudder deflection required for trim for the pylon, small-store, and clean configurations was the same and increased slightly with increase in Mach number. The trend of the rudder deflection required with the large-store configuration was essentially the same except that about 1° more left rudder was required over the Mach number range tested.

The aileron deflection required for trim over the speed range was generally the same for the pylon, small-store, and clean configurations. Below $M \approx 0.9$, the aileron deflection required for these configurations was essentially constant (about 3° right), with a slight trim change present at higher speeds. Below $M = 0.9$, the aileron required to trim the airplane in the large-store configuration was nearly constant and approximately 1° greater than for the other configurations. Above $M \approx 0.9$, an appreciable transonic trim variation, characterized by a left-wing drop, is apparent for this configuration. The trim change above $M \approx 0.9$ probably results from the aggravated compressibility and interference effects with this store configuration, as well as the reduced aileron effectiveness in this speed range.

Lateral dynamic characteristics.- Lateral dynamic characteristics of the airplane with stores were obtained from rudder pulses and are compared to those of the clean airplane (unpublished data) in figure 16. The stores had little effect on the period of the oscillation and slightly decreased the time to damp to one-half amplitude $T_{1/2}$. A slight improvement in the damping ratio is shown for the store configurations and it is apparent that the large-store configuration had the most desirable lateral dynamic characteristics. The pilots could not detect any effects of the stores on the dynamic characteristics of the airplane.

Sideslip characteristics.— Typical examples of sideslip characteristics are presented in figure 17 for Mach numbers of 0.55, 0.80, and 0.98. These basic plots of lateral, directional, and longitudinal control angles and forces, and side force as a function of sideslip angle were essentially linear over the angle-of-sideslip range tested. At the larger angles of sideslip, a negative pitching moment was present that required an increase in δ_e . As the speed increased, the angle of sideslip obtained decreased as a result of the large pedal forces required by the unboosted control system; therefore, only about 1° of sideslip could be obtained on each side of trim at $M \approx 0.98$.

Figure 18 summarizes the sideslip data for the airplane with stores and contains a comparison with the unpublished sideslip characteristics of the clean airplane. The addition of stores increased C_{Y_β} as much as 50 percent. Pylons had little, if any, effect on C_{Y_β} ; however, as the size of the stores increased, C_{Y_β} increased. Values of $dF_r/d\beta$ for the three store configurations tested were the same as for the clean airplane. The apparent directional stability parameter $d\delta_r/d\beta$ was essentially the same for the different configurations, except for a slight increase above $M = 0.9$ for the large-store configuration. The apparent effective dihedral parameter $d\delta_a/d\beta$ for the pylon, small-store configuration, and the clean airplane were the same. Below $M = 0.9$, $d\delta_a/d\beta$ for the airplane in the large-store configuration was slightly greater than for the clean airplane. Above $M \approx 0.94$, $d\delta_a/d\beta$ for the large-store configuration was nearly double the corresponding value for the clean airplane. For all configurations investigated, $d\delta_a/d\beta$ decreased abruptly to a value of about zero at $M \approx 0.92$, and rapidly increased to a value equal to or greater than the subsonic value at $M > 0.92$.

Rolling characteristics.— Figure 19 presents the variation of wing-tip helix angle with aileron deflection for three representative Mach numbers for the large-store configuration. These variations were linear for the control deflections tested and were typical for all configurations.

Figure 20 presents the aileron effectiveness parameter $\frac{pb/2V}{\delta_a}$ over the Mach number range tested and compares these values with unpublished data for the clean airplane. In general, the addition of the stores decreased the value of $\frac{pb/2V}{\delta_a}$ for a given Mach number. An increase in the size of the store resulted in a decrease in $\frac{pb/2V}{\delta_a}$.

The pilots were unable to detect any change in lateral control effectiveness with the various configurations, other than the increase of mass inertia moments with the stores in attempting a rudder-fixed roll.

CONCLUDING REMARKS

The results of a flight investigation, from a Mach number of approximately 0.45 to a Mach number of approximately 1.05, of the Douglas D-558-III research airplane equipped with several configurations of external stores have indicated that the smaller midsemispan store installations generally had a small or negligible effect on the handling qualities of the airplane. With the large-store configuration, the trends exhibited in the longitudinal and lateral trim, stall approach, dynamic and static stability and control, and buffeting characteristics were generally the same as for the clean airplane; however, significant changes in the magnitude of the parameters measured were sometimes apparent, particularly at the higher speeds.

The large-store configuration effected: a decrease in the subsonic static longitudinal stability; an improvement in the lateral damping characteristics at subsonic speed; an appreciable left-wing drop at a Mach number greater than 0.9; an appreciable decrease in lift-curve slope between a Mach number of about 0.85 and 0.96; a slight decrease in the level of lift for the onset of buffeting at all subsonic speeds; and an appreciable increase in apparent dihedral parameter $d\delta_a/d\beta$ particularly at a Mach number greater than 0.94. The side-force parameter $C_{Y\beta}$ increased and the aileron control effectiveness parameter $\frac{pb/2V}{\delta_a}$ decreased with an increase in the size of the stores.

High-Speed Flight Station,
National Advisory Committee for Aeronautics,
Edwards, Calif., July 30, 1957.

REFERENCES

1. Silvers, H. Norman, and King, Thomas J., Jr.: Investigation at High Subsonic Speeds of the Effects of Various Underwing External-Store Arrangements on the Aerodynamic Characteristics of a 1/16-Scale Model of the Douglas D-558-II Research Airplane. NACA RM L55D11, 1955.
2. Smith, Norman F.: Exploratory Investigation of External Stores on the Aerodynamic Characteristics of a 1/16-Scale Model of the Douglas D-558-II Research Airplane at a Mach Number of 2.01. NACA RM L54F02, 1954.
3. Carmel, Melvin M., and Turner, Kenneth L.: Investigation of Drag and Static Longitudinal and Lateral Stability Characteristics of a Model of a 40.4° Swept-Wing Airplane at Mach Numbers of 1.56 and 2.06. NACA RM L56I17a, 1957.
4. Alford, William J., Jr., Silvers, H. Norman, and King, Thomas J., Jr.: Preliminary Low-Speed Wind-Tunnel Investigation of Some Aspects of the Aerodynamic Problems Associated With Missiles Carried Externally in Positions Near Airplane Wings. NACA RM L54J20, 1954.
5. Nugent, Jack: Effect of Wing-Mounted External Stores on the Lift and Drag of the Douglas D-558-II Research Airplane at Transonic Speeds. NACA RM H57E15a, 1957.
6. Fischel, Jack, and Reisert, Donald: Effect of Several Wing Modifications on the Subsonic and Transonic Longitudinal Handling Qualities of the Douglas D-558-II Research Airplane. NACA RM H56C30, 1956.
7. Wolowicz, Chester H., and Rediess, Herman A.: Effects of Jet Exhausts on Flight-Determined Longitudinal and Lateral Dynamic Stability Characteristics of the Douglas D-558-II Research Airplane. NACA RM H57G09, 1957.
8. Fischel, Jack, and Reisert, Donald: Effect of Several Wing Modifications on the Low-Speed Stalling Characteristics of the Douglas D-558-II Research Airplane. NACA RM H55E31a, 1955.

TABLE I.- PHYSICAL CHARACTERISTICS OF THE DOUGLAS D-558-II AIRPLANE

Wing:

Root airfoil section (normal to 30-percent chord of unswept panel)	NACA 63-010
Tip airfoil section (normal to 30-percent chord of unswept panel)	NACA 63 ₁ -012
Total area, sq ft	175
Span, ft	25
Mean aerodynamic chord, in.	87.301
Root chord (parallel to plane of symmetry), in.	108.51
Tip chord (parallel to plane of symmetry), in.	61.18
Taper ratio	0.565
Aspect ratio	3.57
Sweep at 30-percent chord of unswept panel, deg	35
Sweep of leading edge, deg	38.8
Incidence at fuselage center line, deg	3
Dihedral, deg	-3
Geometric twist, deg	0
Total aileron area (rearward of hinge line), sq ft	9.8
Aileron travel (each), deg	±15
Total flap area, sq ft	12.58
Flap travel, deg	50

Horizontal tail:

Root airfoil section (normal to 30-percent chord of unswept panel)	NACA 63-010
Tip airfoil section (normal to 30-percent chord of unswept panel)	NACA 63-010
Area (including fuselage), sq ft	39.9
Span, in.	143.6
Mean aerodynamic chord, in.	41.75
Root chord (parallel to plane of symmetry), in.	53.6
Tip chord (parallel to plane of symmetry), in.	26.8
Taper ratio	0.50
Aspect ratio	3.59
Sweep at 30-percent chord line of unswept panel, deg	40
Dihedral, deg	0
Elevator area, sq ft	9.4
Elevator travel, deg	
Up	25
Down	15
Stabilizer travel, deg	
Leading edge up	4
Leading edge down	5

Vertical tail:

Airfoil section (normal to 30-percent chord of unswept panel)	NACA 63-010
Area, sq ft	36.6
Height from fuselage center line, in.	98
Root chord (parallel to fuselage center line), in.	146
Tip chord (parallel to fuselage center line), in.	44
Sweep angle at 30-percent chord of unswept panel, deg	49
Rudder area (rearward of hinge line), sq ft	6.15
Rudder travel, deg	±25

Fuselage:

Length, ft	42
Maximum diameter, in.	60
Fineness ratio	8.40
Speed-retarder area, sq ft	5.25

Engines:

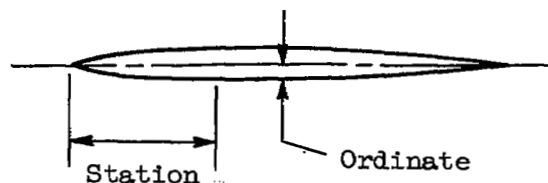
Turbojet	J-34-WE-40
Rocket	LR8-RM-6

Airplane weight, lb:

Full jet and rocket fuel	15,570
Full jet fuel	12,382
No fuel	10,822

TABLE II.- CROSS-SECTIONAL DIMENSIONS OF PYLON

[Stations and ordinates given in inches]

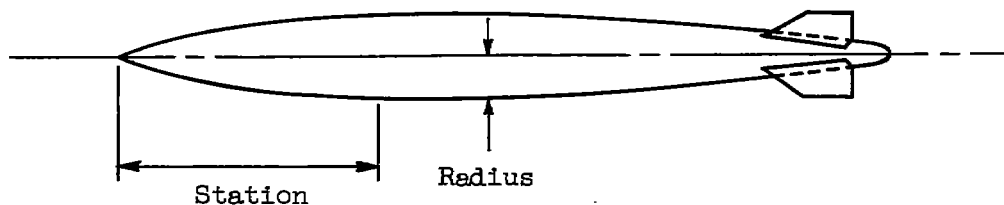


Station	Ordinate	Station	Ordinate
0	0	30.0	2.50
.5	.51	32.5	2.50
1.0	.72	38.5	2.50
2.5	1.11	41.0	2.48
5.0	1.53	43.5	2.42
7.5	1.82	46.0	2.31
10.0	2.04	48.5	2.15
12.5	2.21	51.0	1.94
15.0	2.34	53.5	1.68
17.5	2.43	58.5	1.05
20.0	2.48	63.5	.34
22.5	2.50	66.0	0
25.0	2.50		
27.5	2.50		
L.E. radius: 0.275			
T.E. radius: 0.045			

TABLE III.- DIMENSIONS OF SMALL STORES

(DAC 1,000-POUND BOMB)

[Stations and radii given in inches]

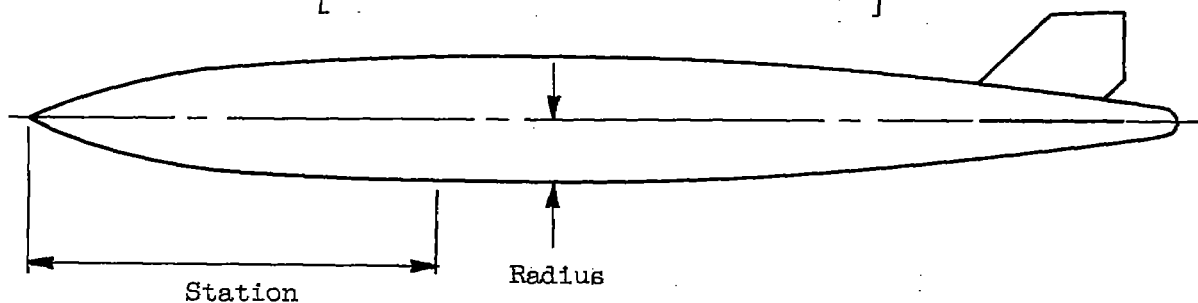


Station	Radius	Station	Radius
0	0	73.0	6.61
4	1.83	79.7	6.15
9.0	3.44	86.3	5.55
15.7	4.82	93.0	4.83
22.3	5.69	98.7	4.14
29.0	6.33	102.0	3.72
35.7	6.79	105.3	3.28
42.3	7.00	108.7	2.83
48.0	7.00	112.3	2.33
54.7	7.00	115.0	1.96
59.7	7.00	117.7	1.45
66.3	6.90	120.0	0
L.E. slope: $\text{Tan} = 0.531$			
L.E. radius: 0.25			
T.E. radius: 0.75			

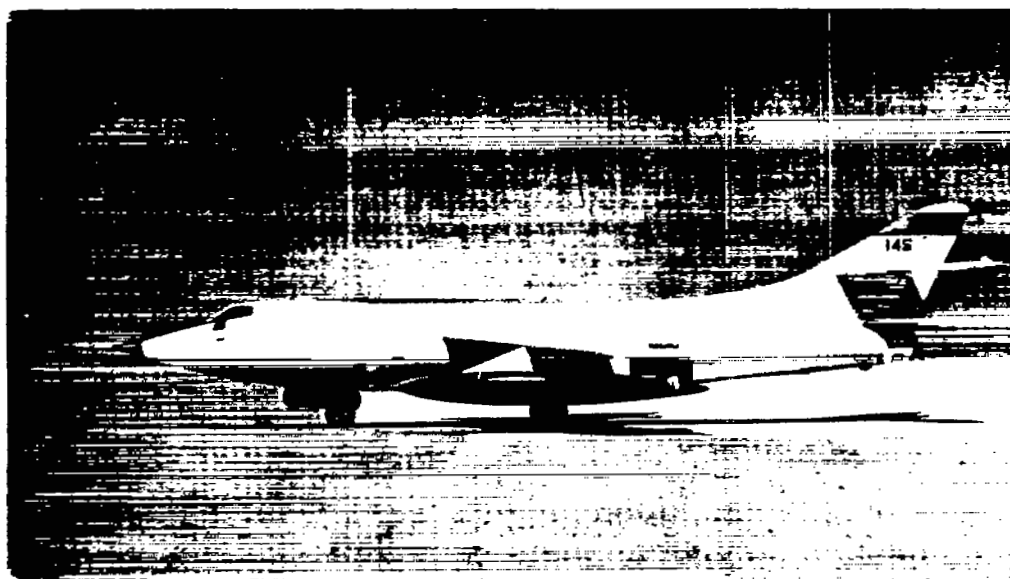
TABLE IV.- DIMENSIONS OF LARGE STORES

(DAC 150-GALLON FUEL TANK)

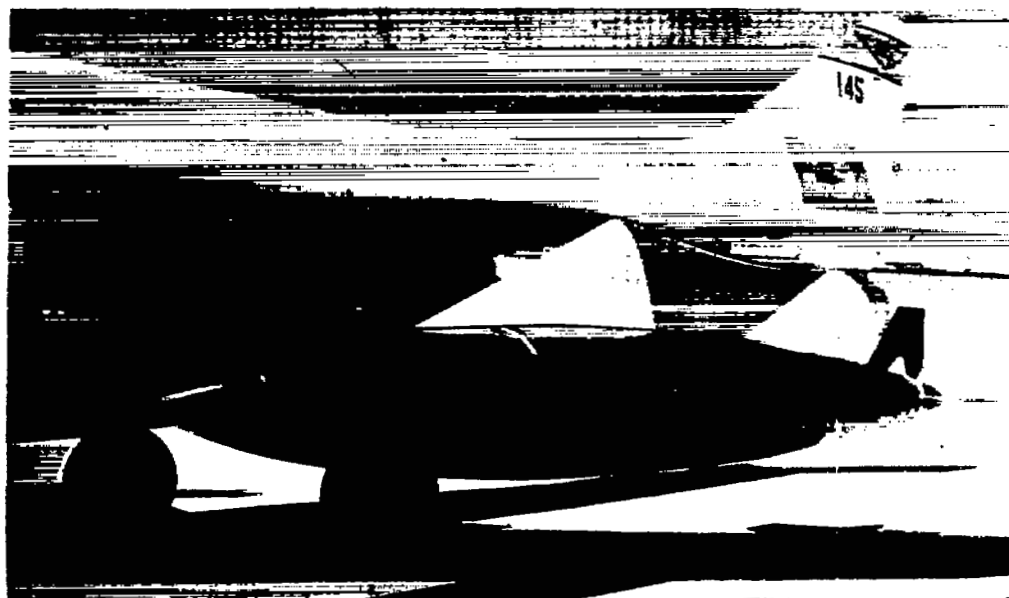
[Stations and radii given in inches]



Station	Radius	Station	Radius
0	0	109.5	9.91
6	2.75	119.5	9.23
13.5	5.17	129.5	8.32
23.5	7.23	139.5	7.24
33.5	8.54	148.0	6.22
43.5	9.49	153.0	5.58
53.5	10.19	158.0	4.92
63.5	10.50	163.0	4.25
73.5	10.50	168.5	3.50
83.5	10.50	172.5	2.93
89.5	10.50	176.5	2.17
99.5	10.35	180.0	0
L.E. slope: $\tan = 0.531$			
L.E. radius: 1.00			
T.E. radius: 1.00			



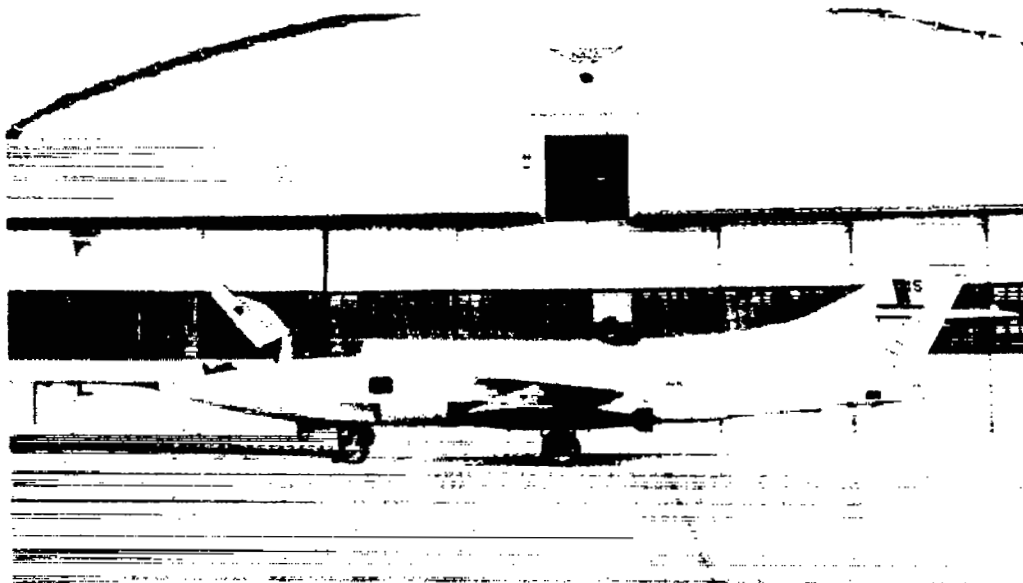
E-1861



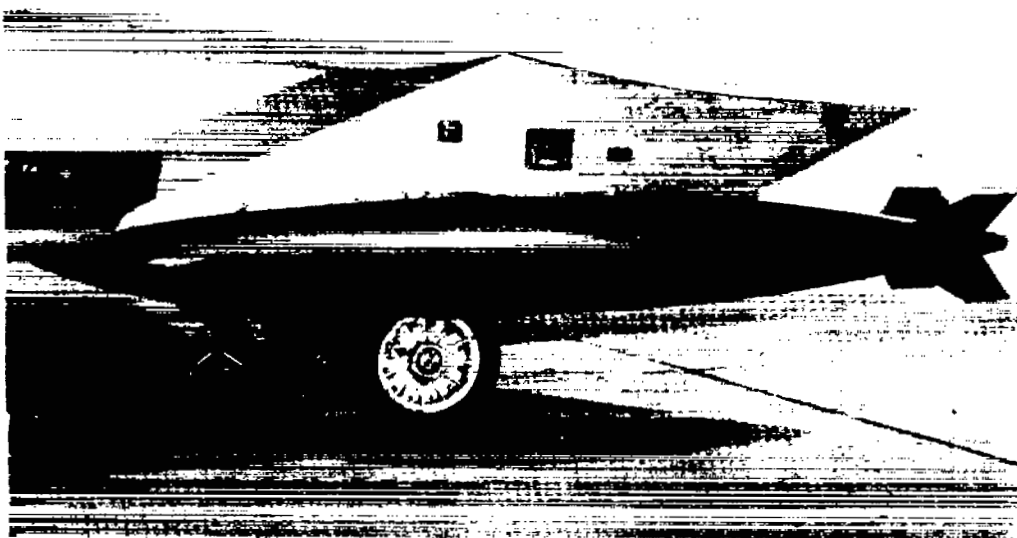
E-1866

(a) Large-store configuration.

Figure 1.- Photographs of stores configurations investigated.



E-1161



(b) Small-store configuration.

E-1164

Figure 1.- Concluded.

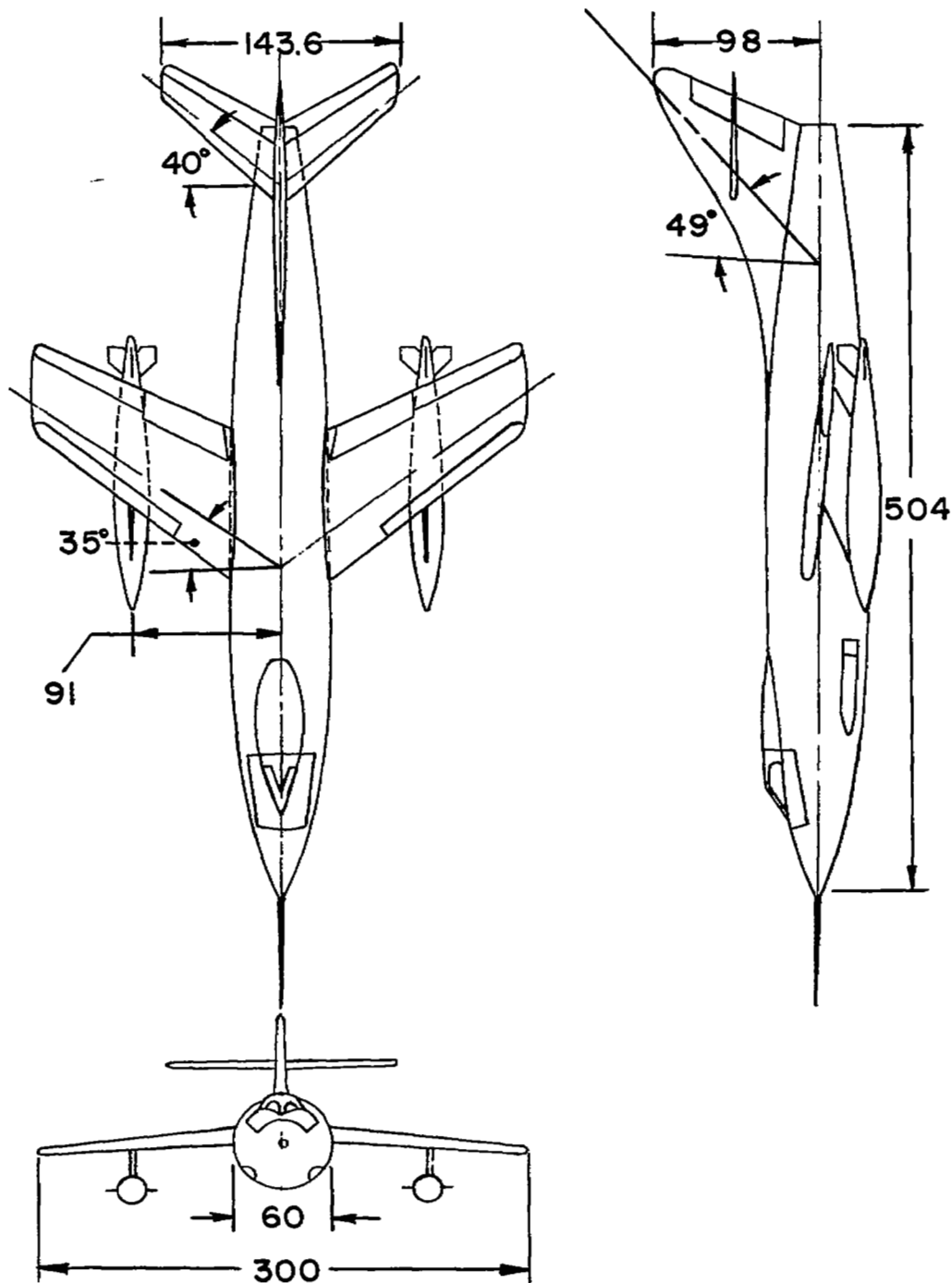
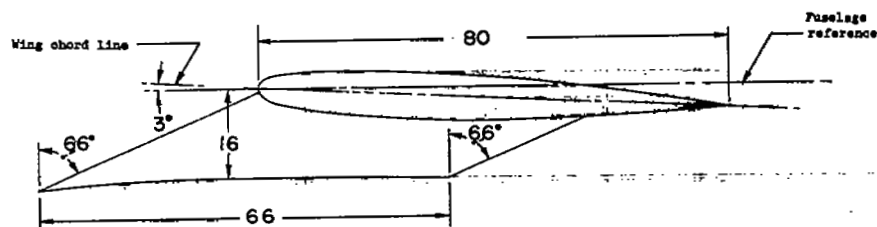
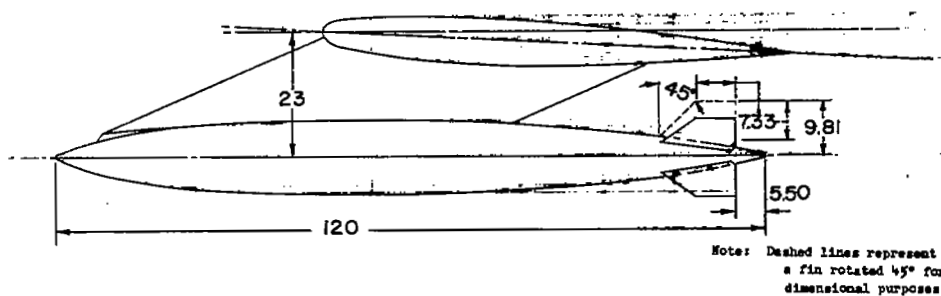


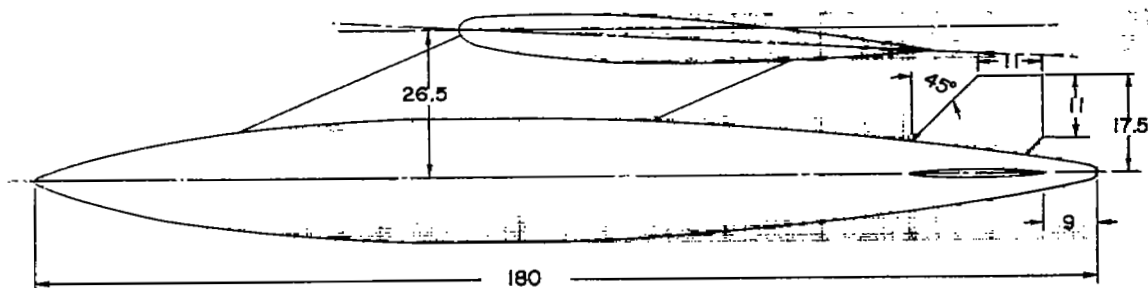
Figure 2.- Three-view drawing of the airplane in the large-store configuration. All dimensions in inches.



(a) Pylon configuration.



(b) Small-store configuration.



(c) Large-store configuration.

Figure 3.- Details of each store configuration investigated. All dimensions in inches.

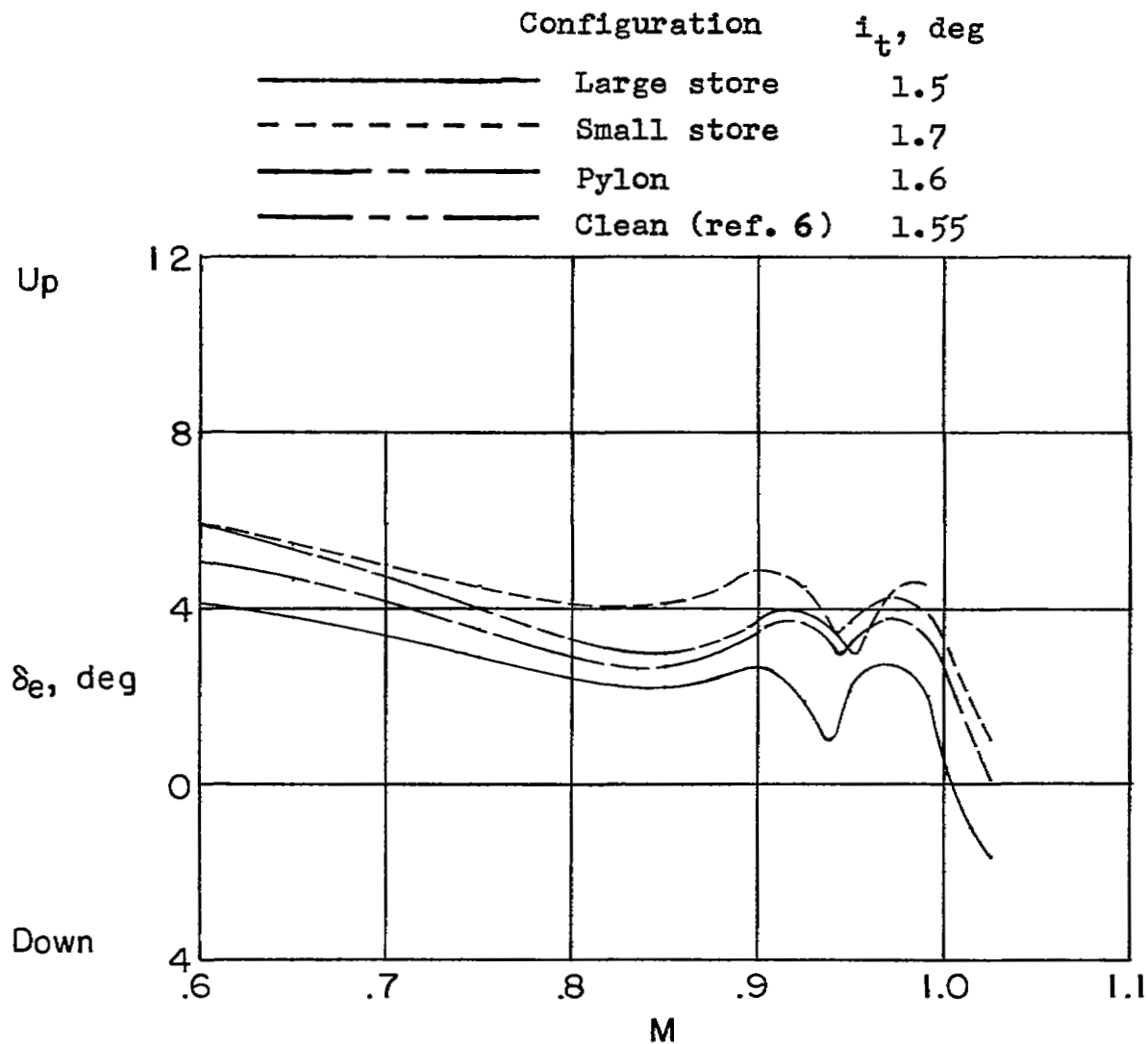


Figure 4.- Elevator deflection required for longitudinal trim for all configurations tested. D-558-II airplane; $h_p = 35,000$ feet; $W = 13,000$ pounds; $a_n = 1.0$.

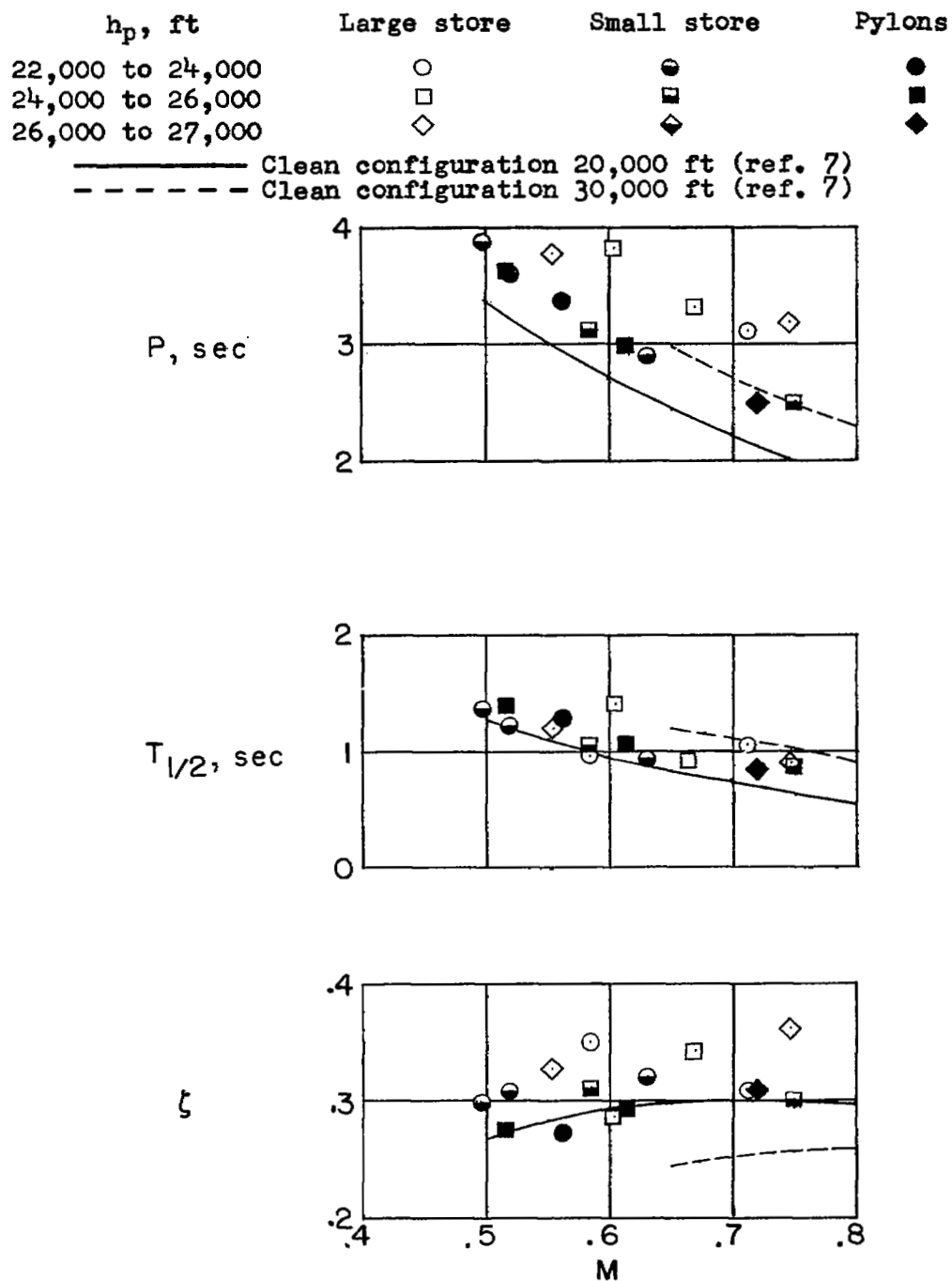
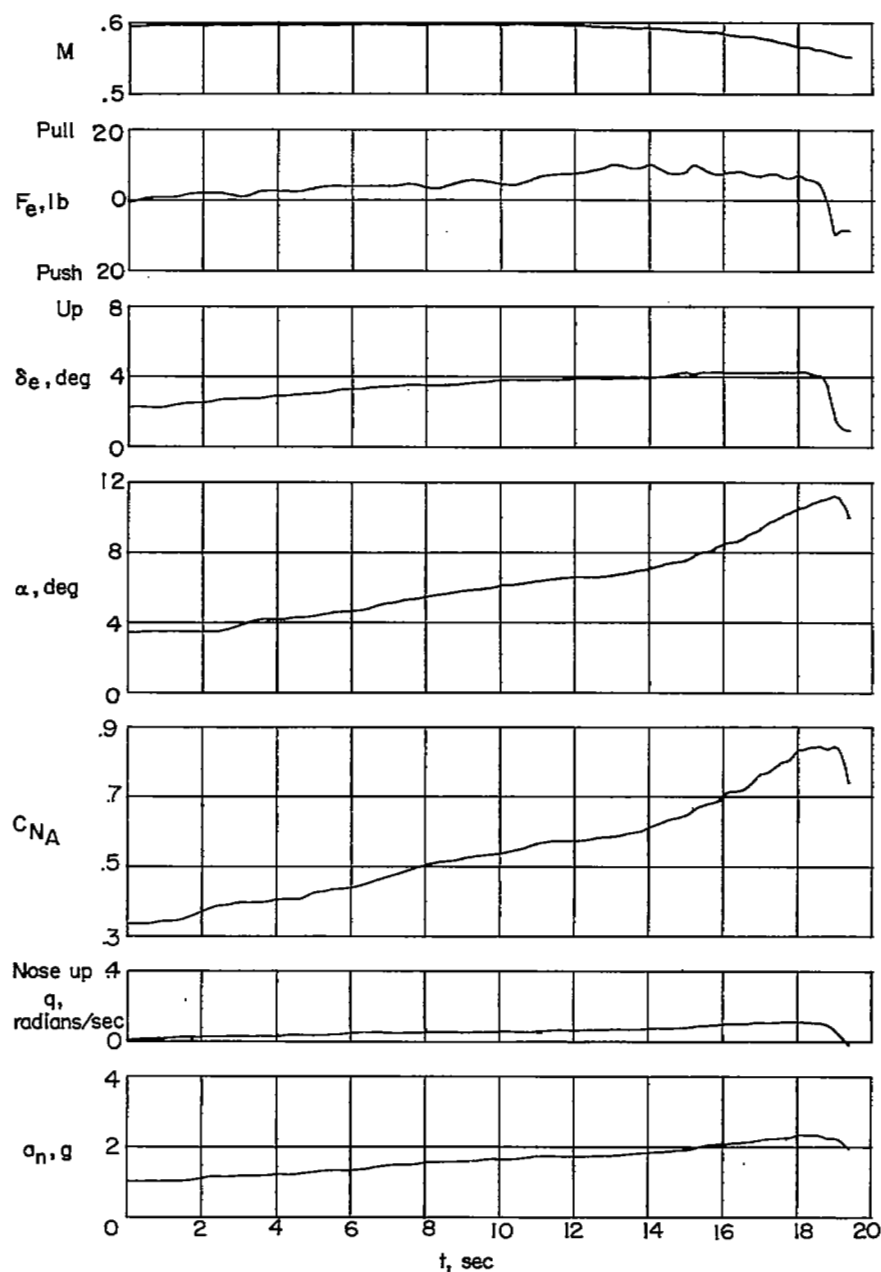
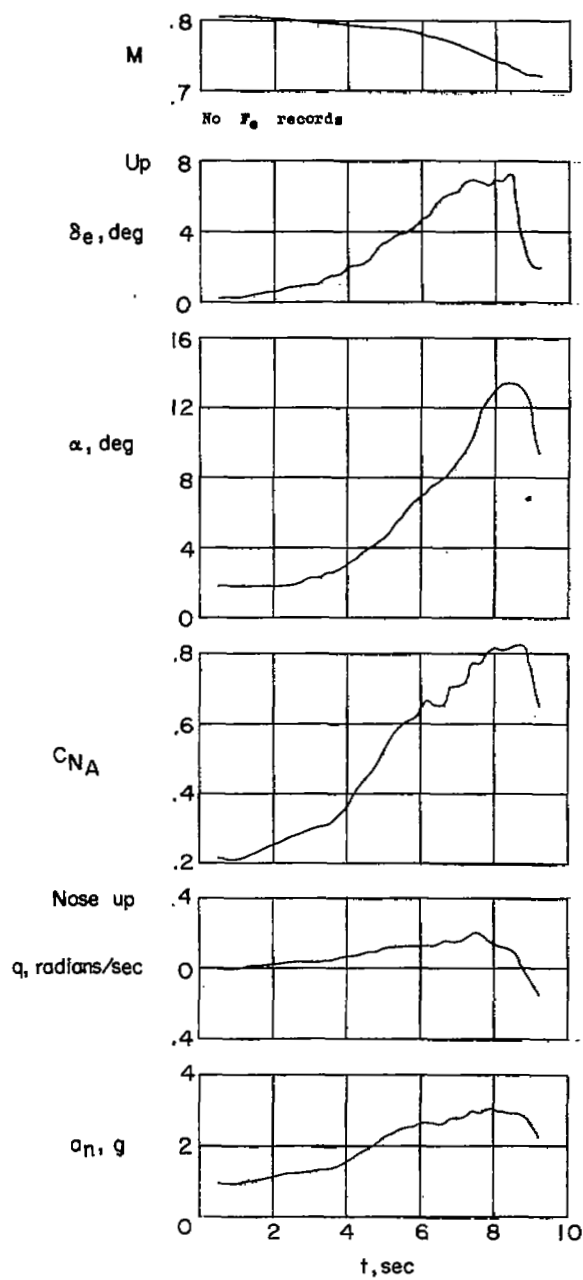


Figure 5.- Dynamic longitudinal characteristics for all configurations tested. D-558-II airplane.



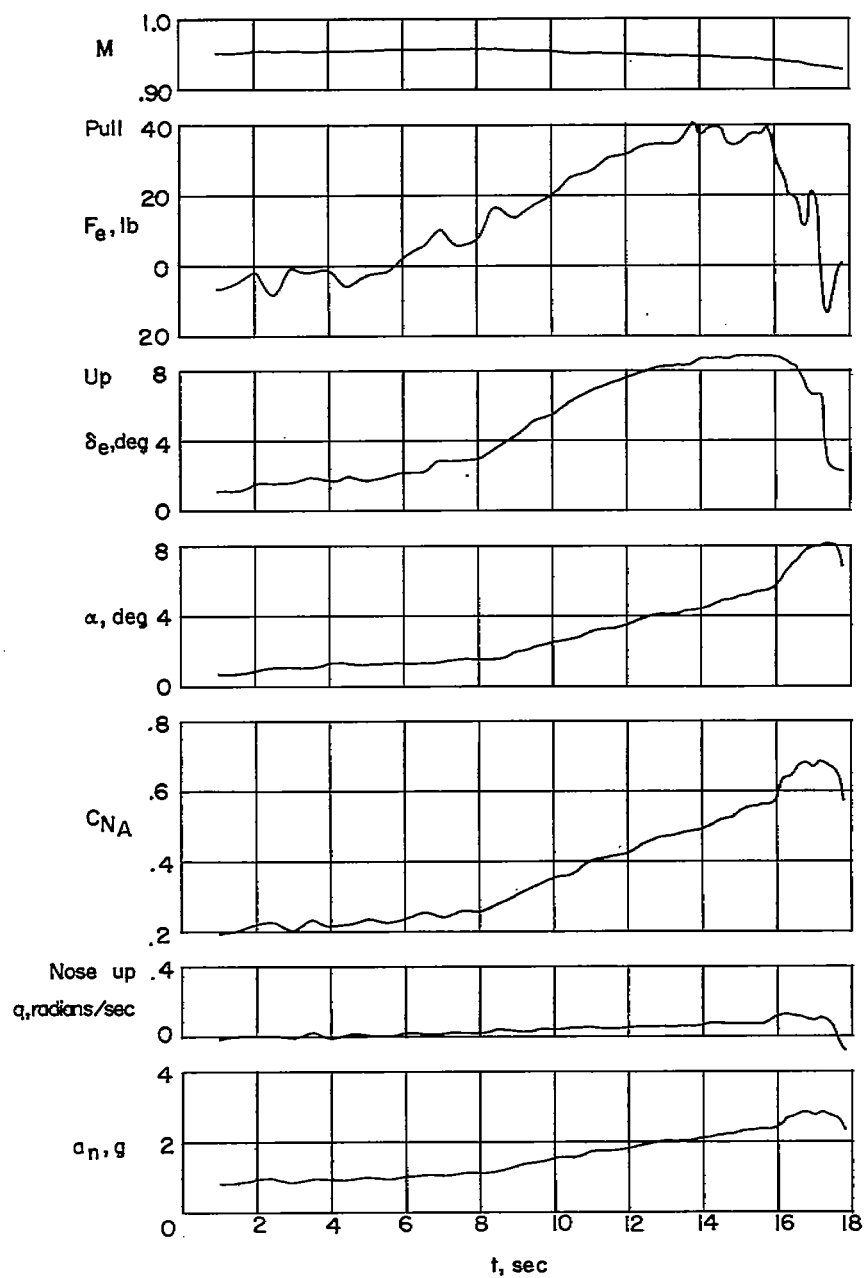
(a) $M \approx 0.60$; $h_p \approx 23,500$ feet; $i_t = 1.70^\circ$.

Figure 6.- Representative time histories of wind-up turns performed with the D-558-II airplane in the large-store configuration.



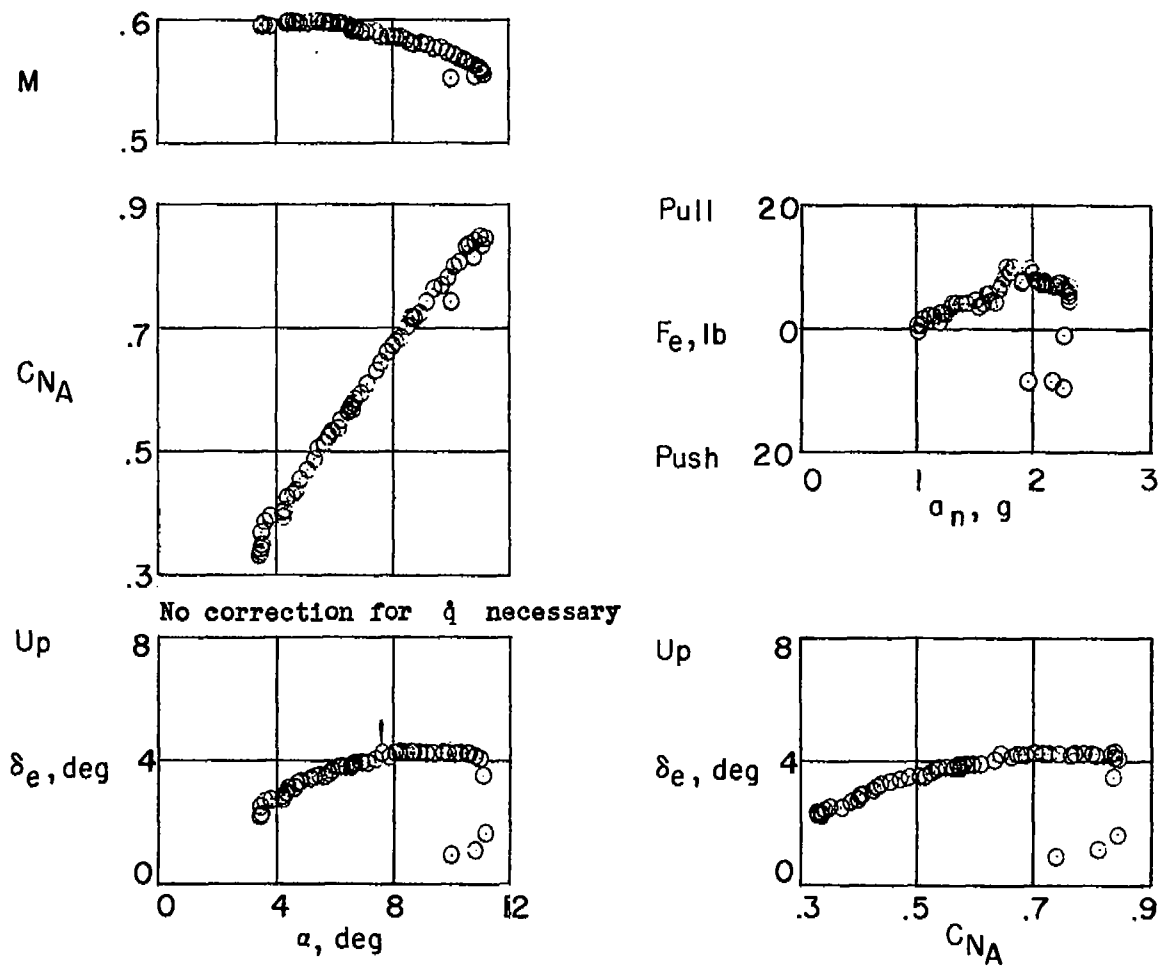
(b) $M \approx 0.80$; $h_p \approx 28,700$ feet; $i_t = 1.55^\circ$.

Figure 6.- Continued.



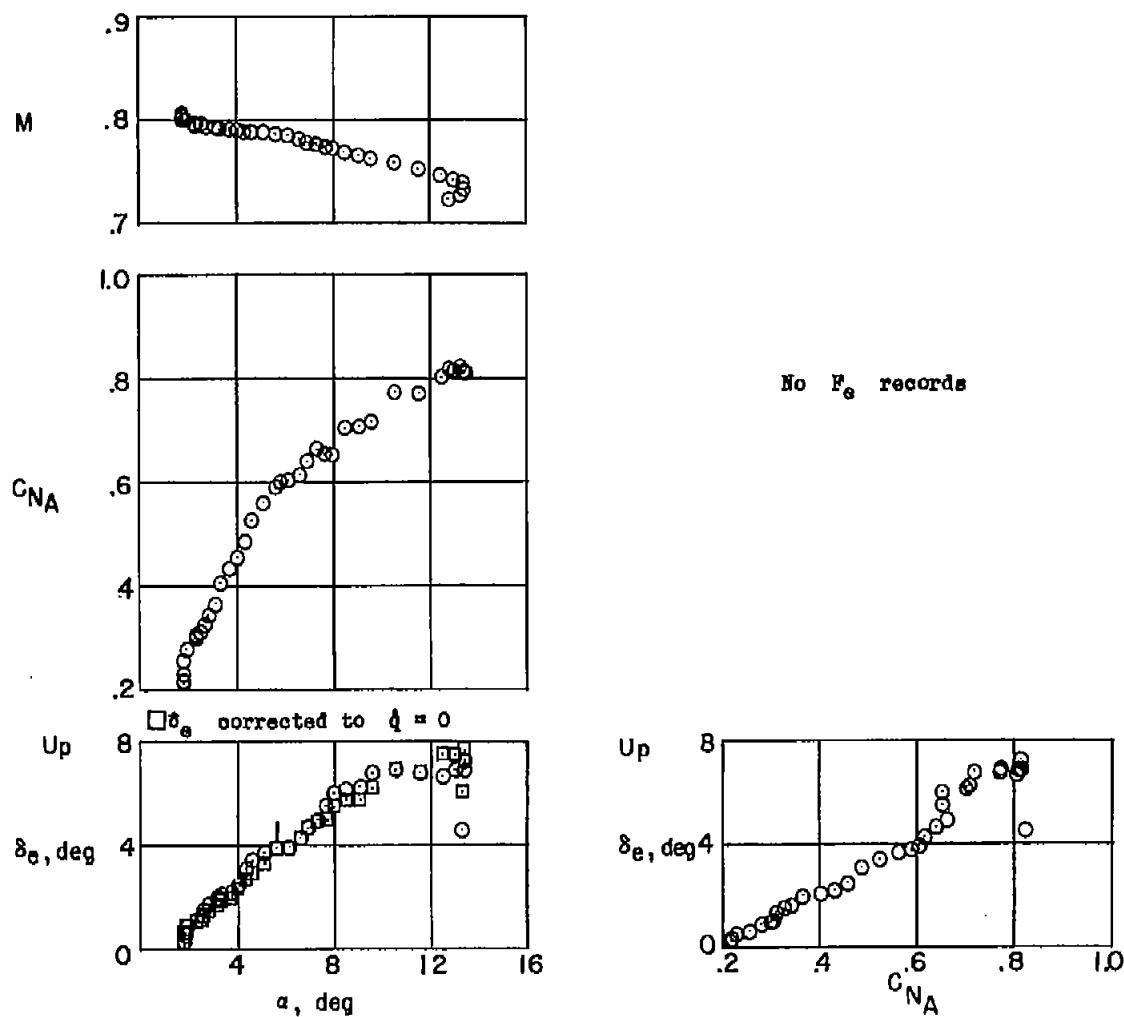
(c) $M \approx 0.95$; $h_p \approx 34,000$ feet; $i_t = 1.80^\circ$.

Figure 6.- Concluded.



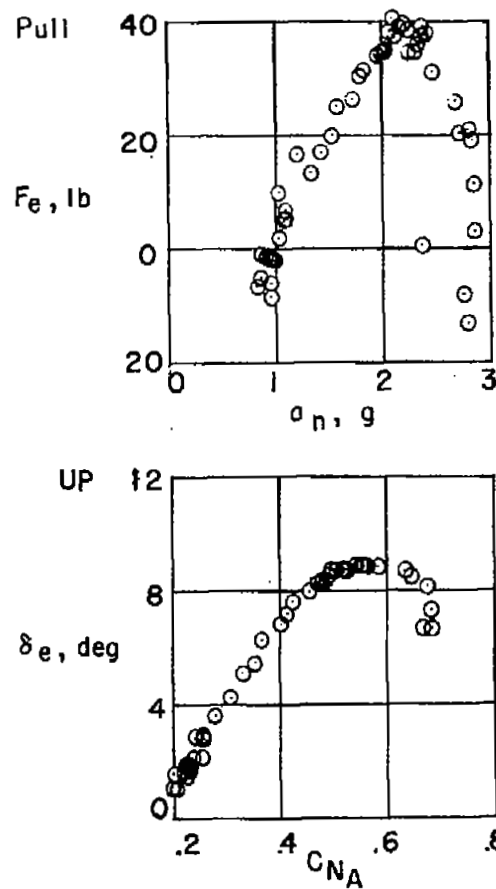
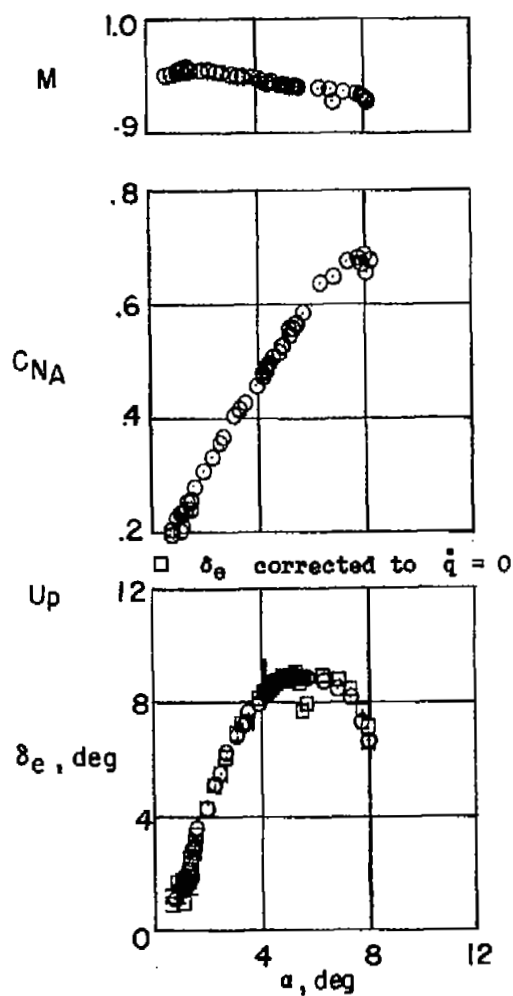
(a) $M \approx 0.60$; $h_p \approx 23,500$ feet; $i_t = 1.70^\circ$.

Figure 7.- Representative stability plots of wind-up turns performed with the D-558-II airplane in the large-store configuration.



(b) $M \approx 0.80$; $h_p \approx 28,700$ feet; $i_t = 1.55^\circ$.

Figure 7.- Continued.



(c) $M \approx 0.95$; $h_p \approx 34,000$ feet; $i_t = 1.80^\circ$.

Figure 7.- Concluded.

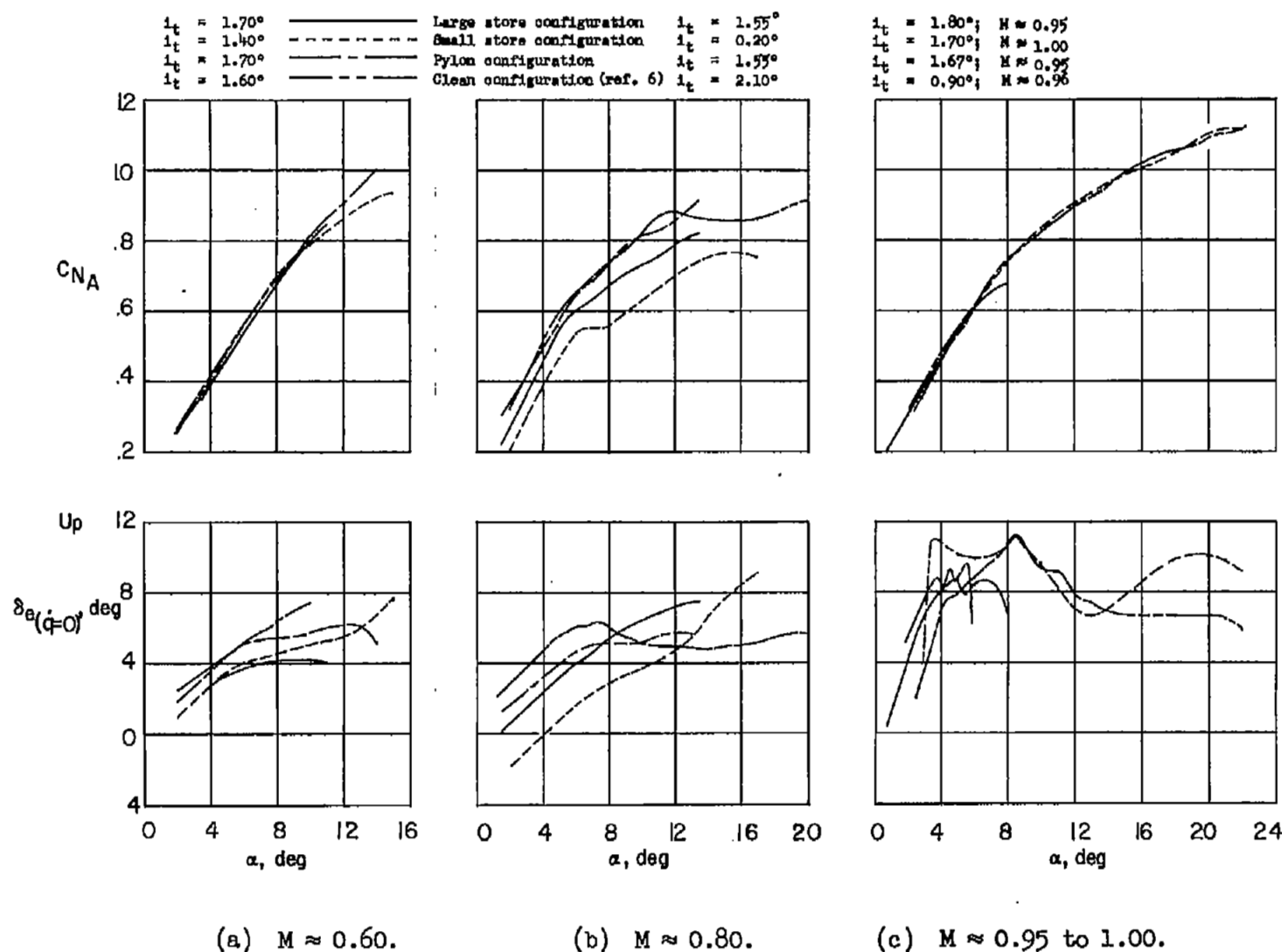


Figure 8.- Comparison of normal force and apparent stability characteristics of the D-558-II airplane for the configurations tested.

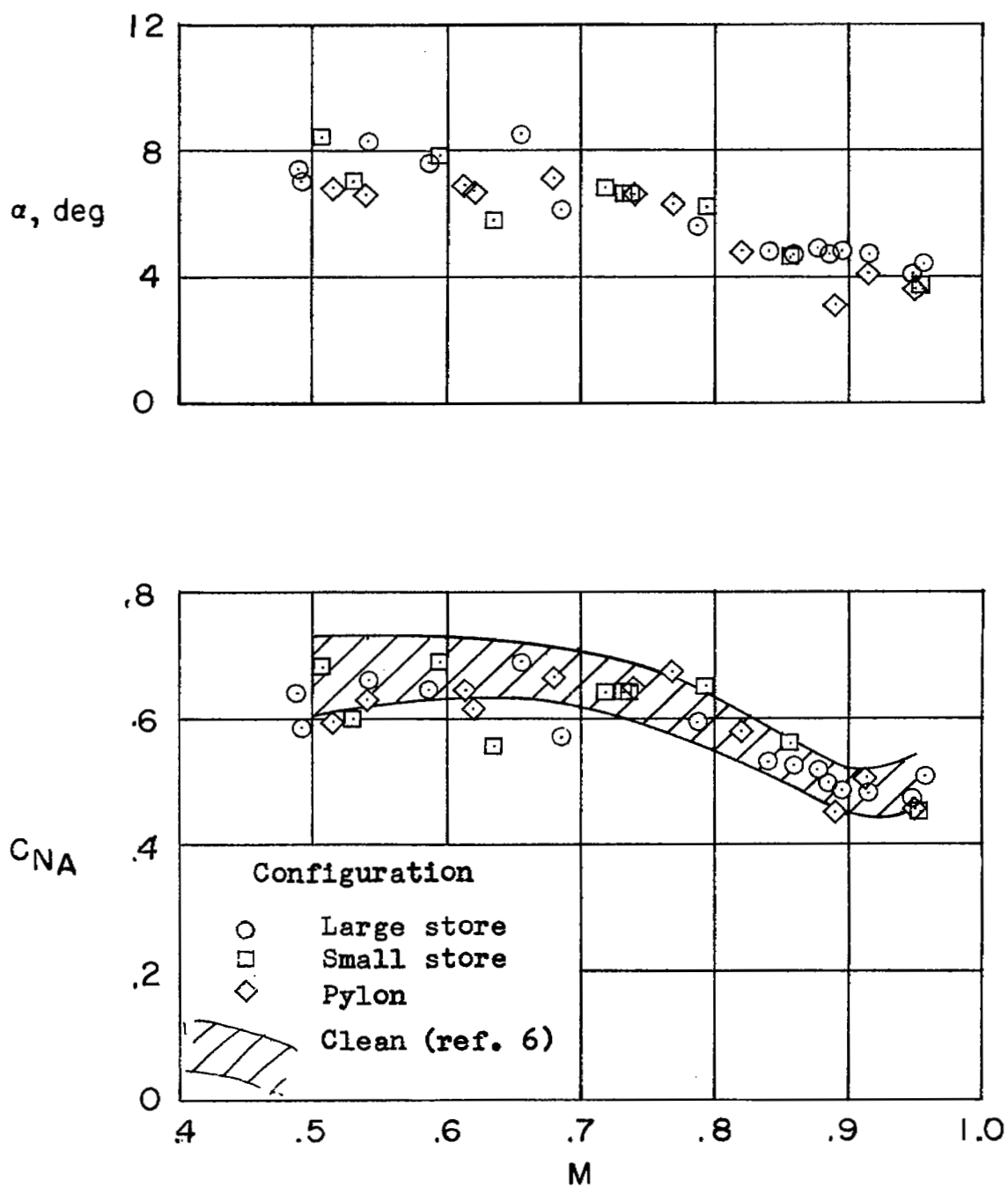


Figure 9.- Boundary for decreased stability of the D-558-II airplane for all configurations tested.

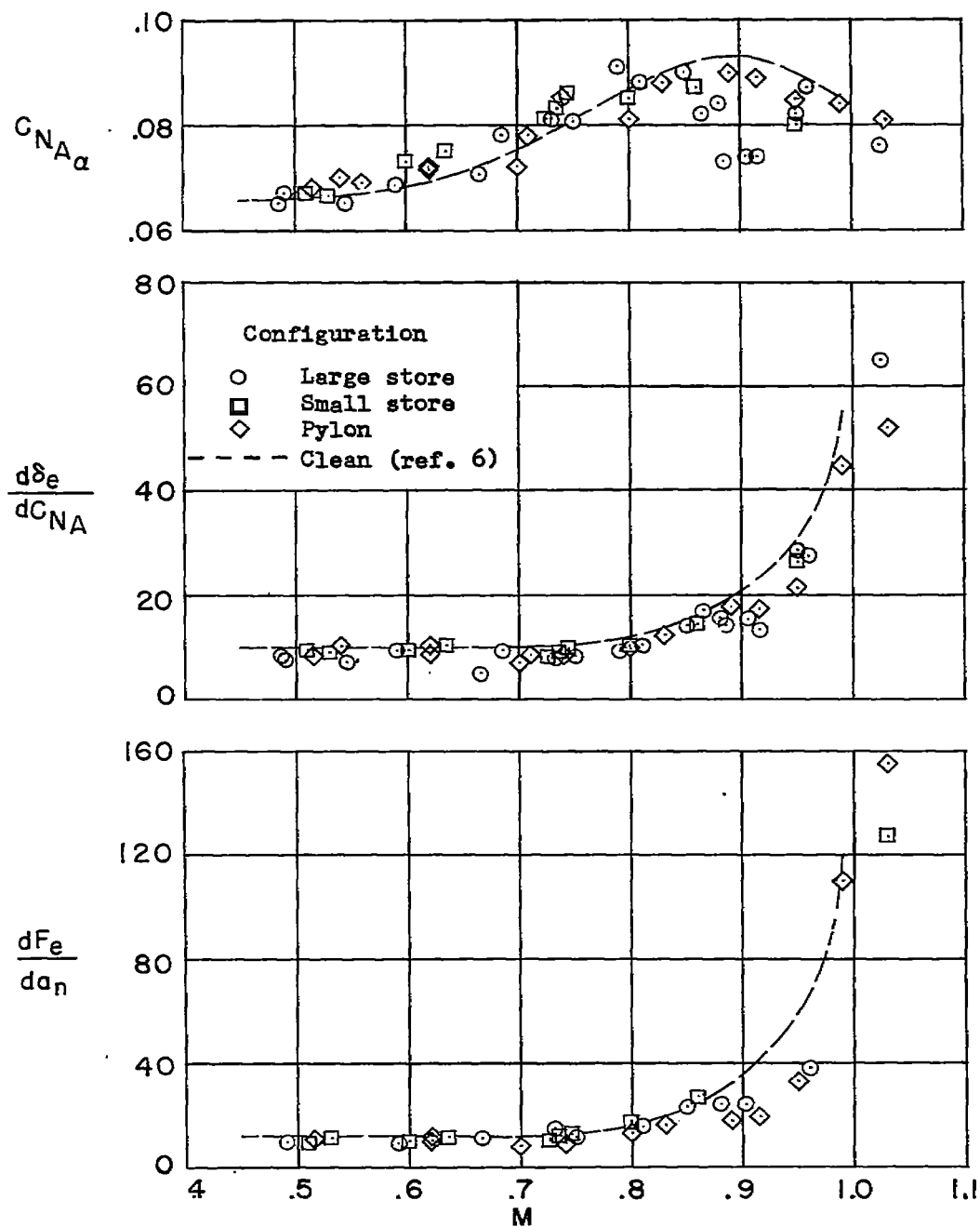


Figure 10.- Comparison of the longitudinal stability and control effectiveness parameters of the D-558-II airplane for the configurations tested.

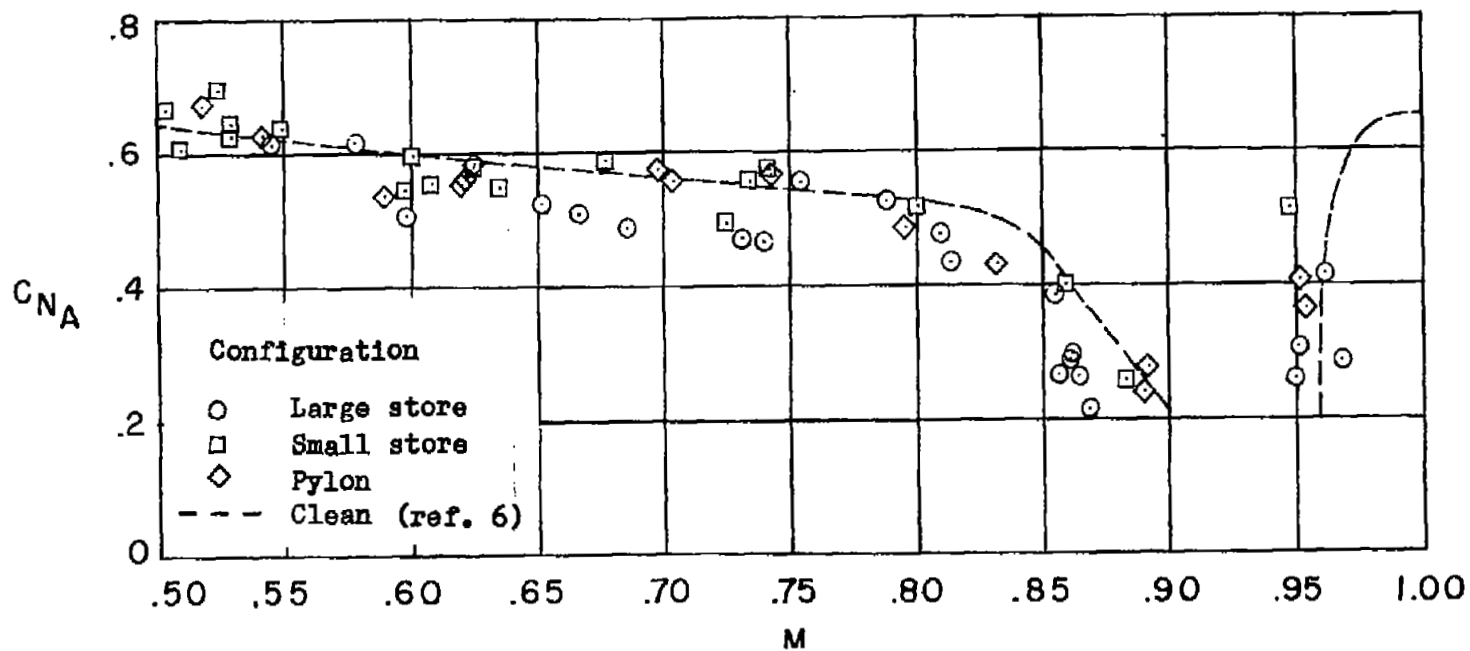
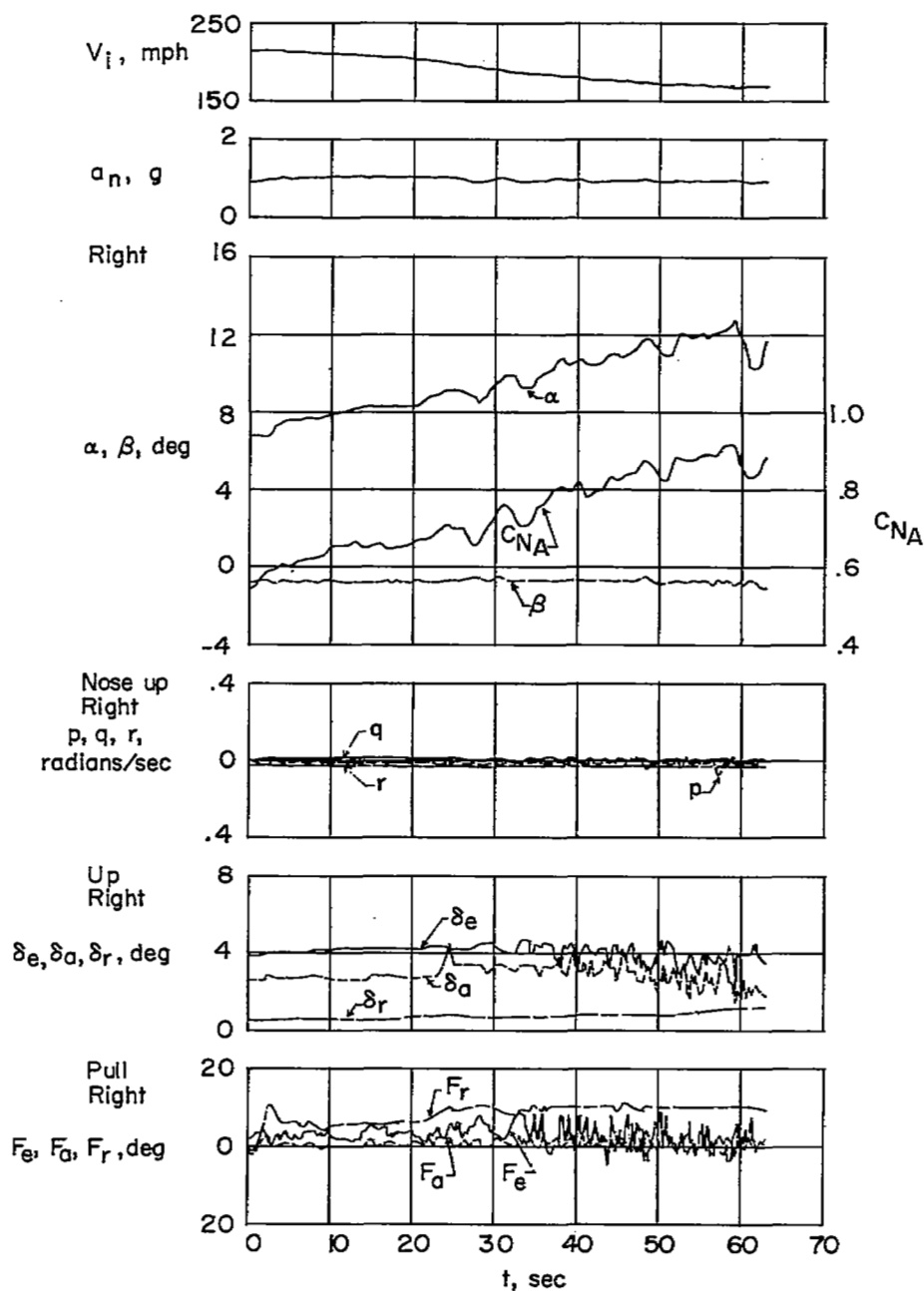
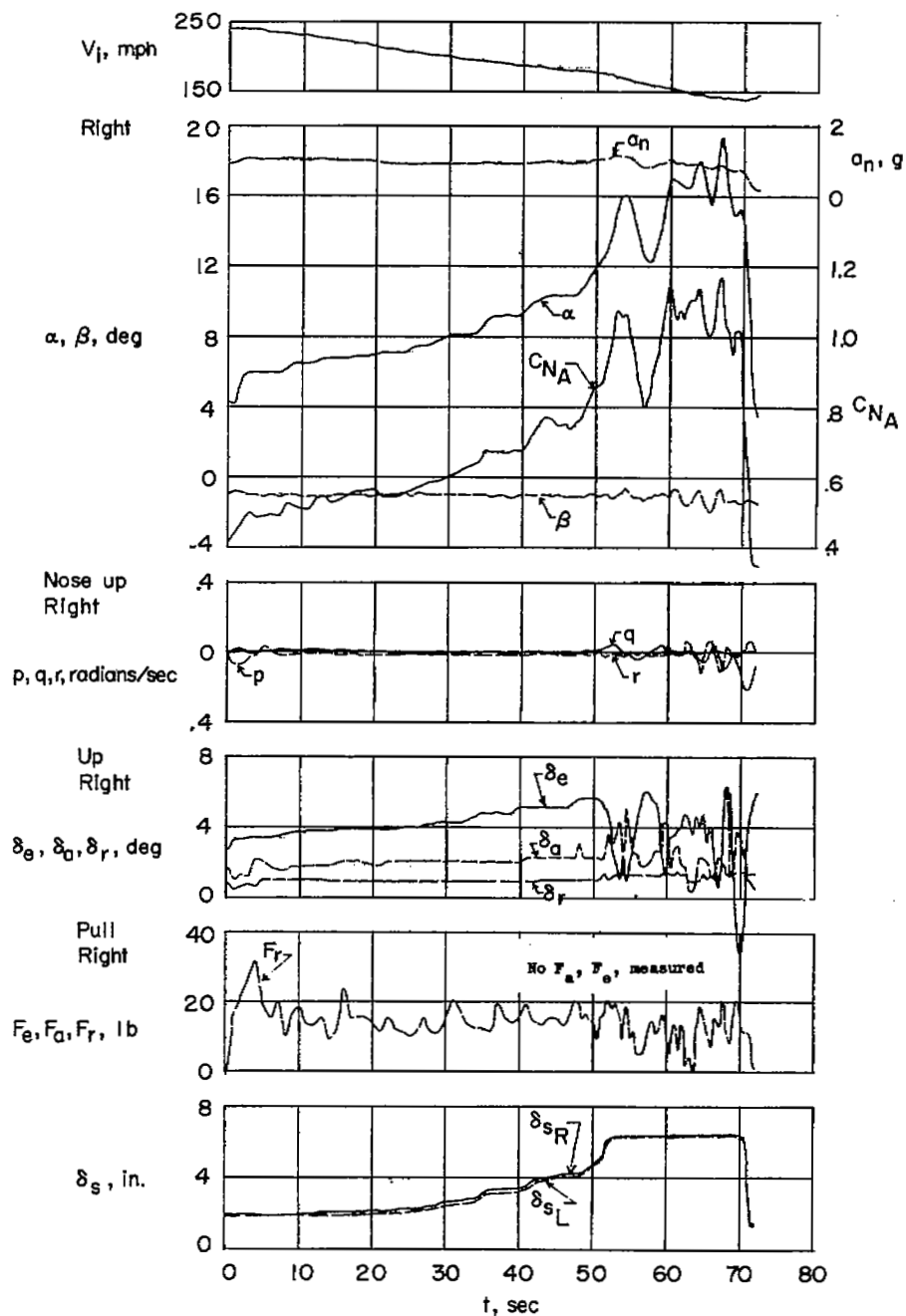


Figure 11.- Buffet boundary of the D-558-II airplane for the configurations tested.



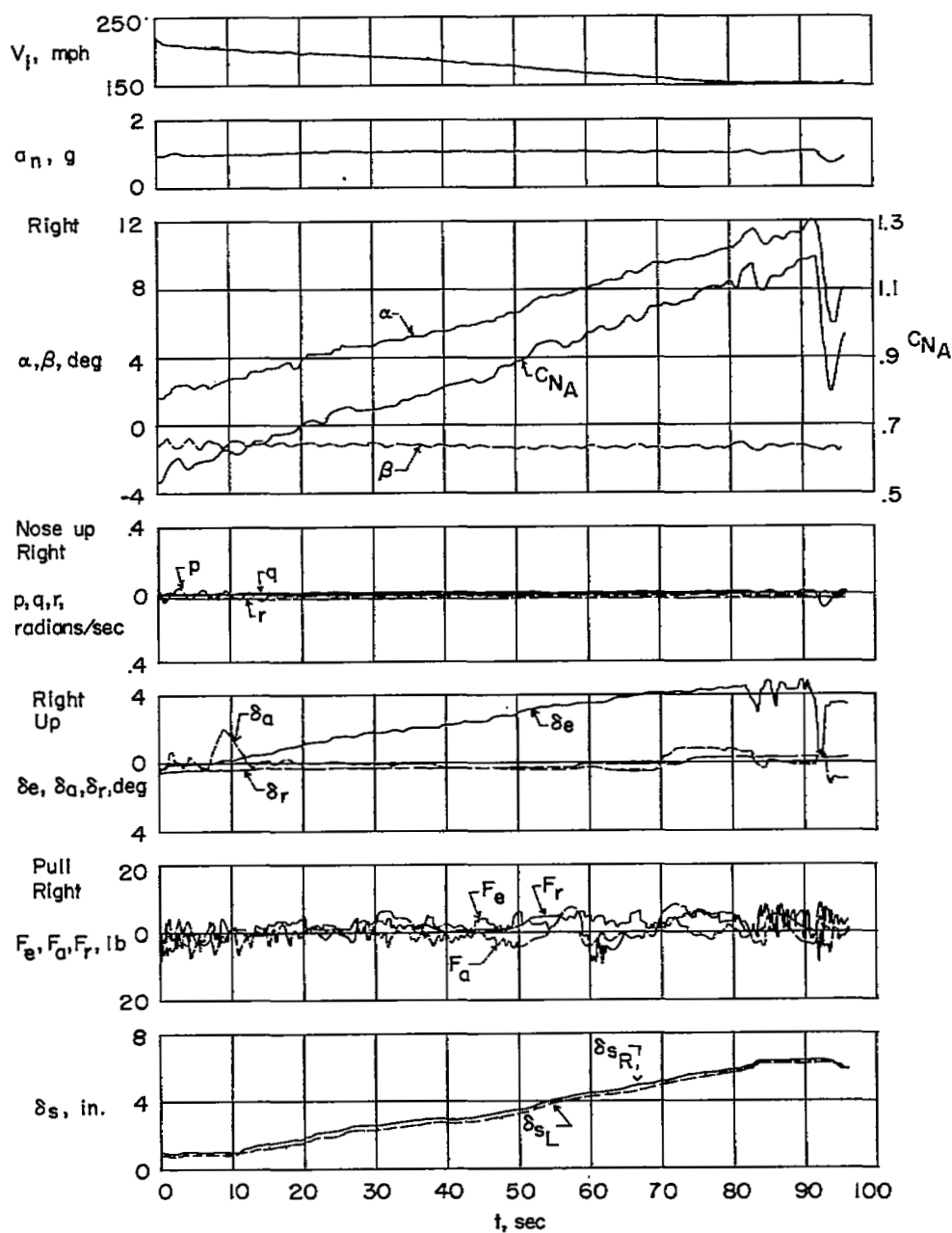
(a) Slats-locked condition.

Figure 12.- Typical time histories of stall approaches performed with the D-558-II airplane in the large-store configuration.



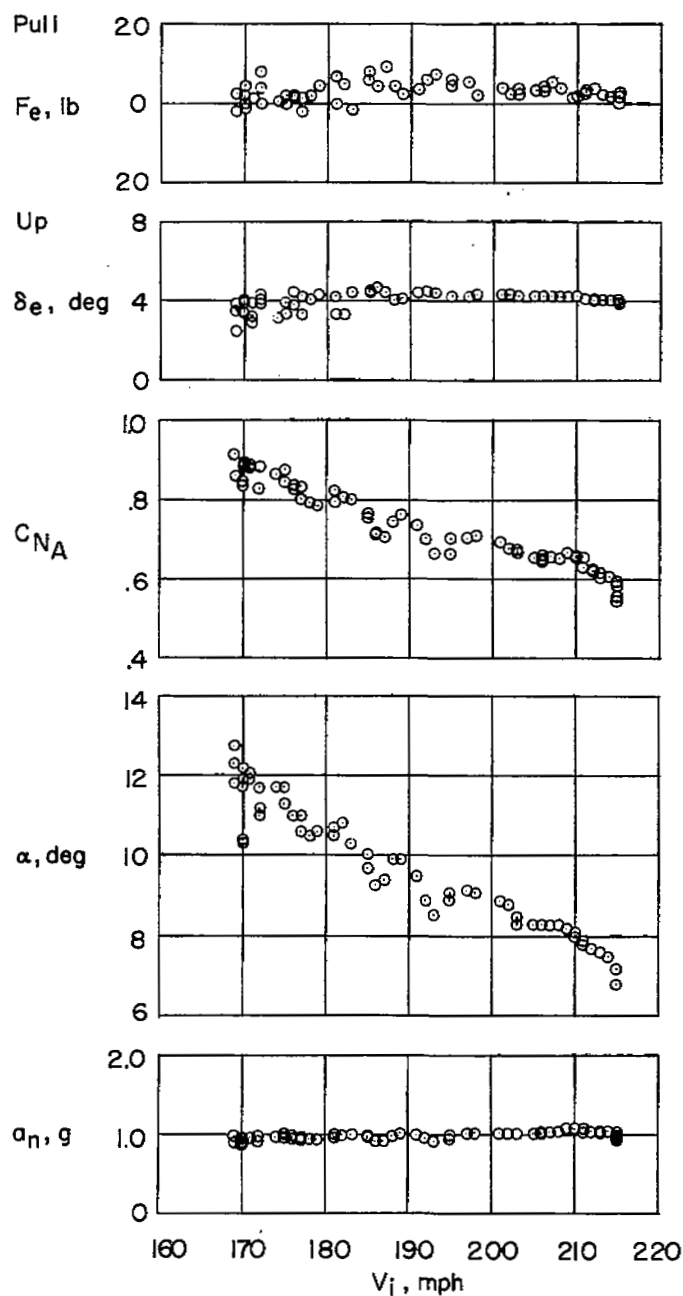
(b) Slats-unlocked condition.

Figure 12.- Continued.



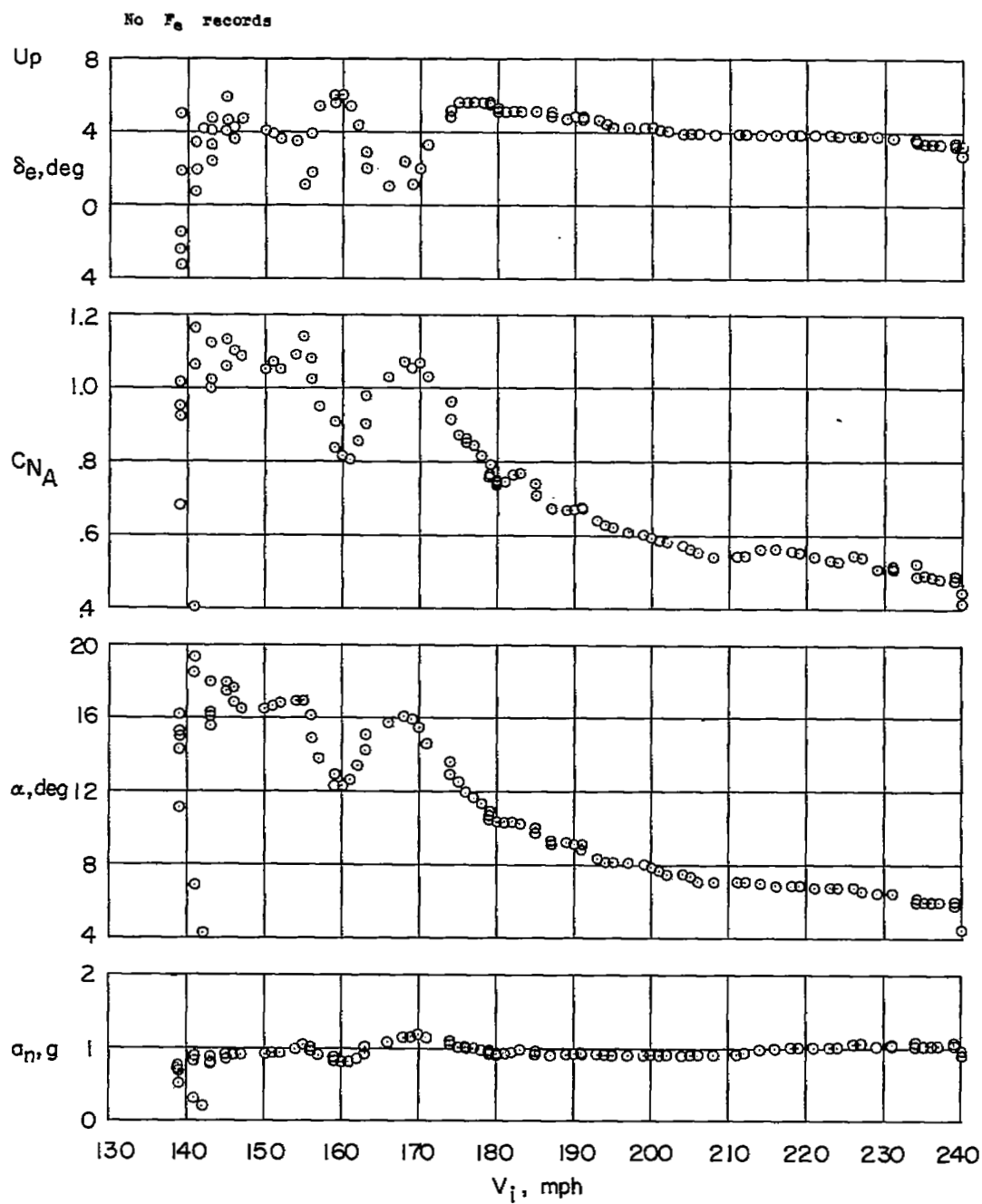
(c) Landing condition.

Figure 12.- Concluded.



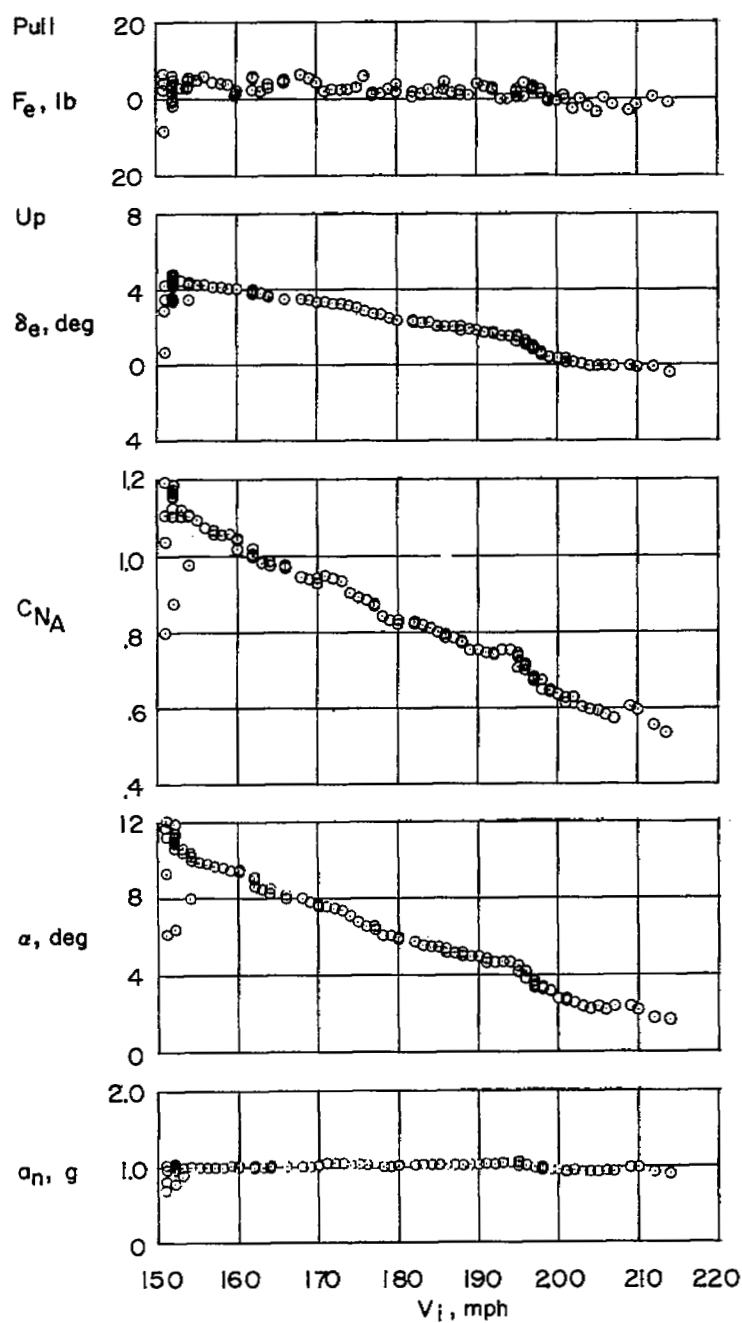
(a) Slats-locked condition.

Figure 13.- Typical stability plots of stall approaches performed with the D-558-II airplane in the large-store configuration.



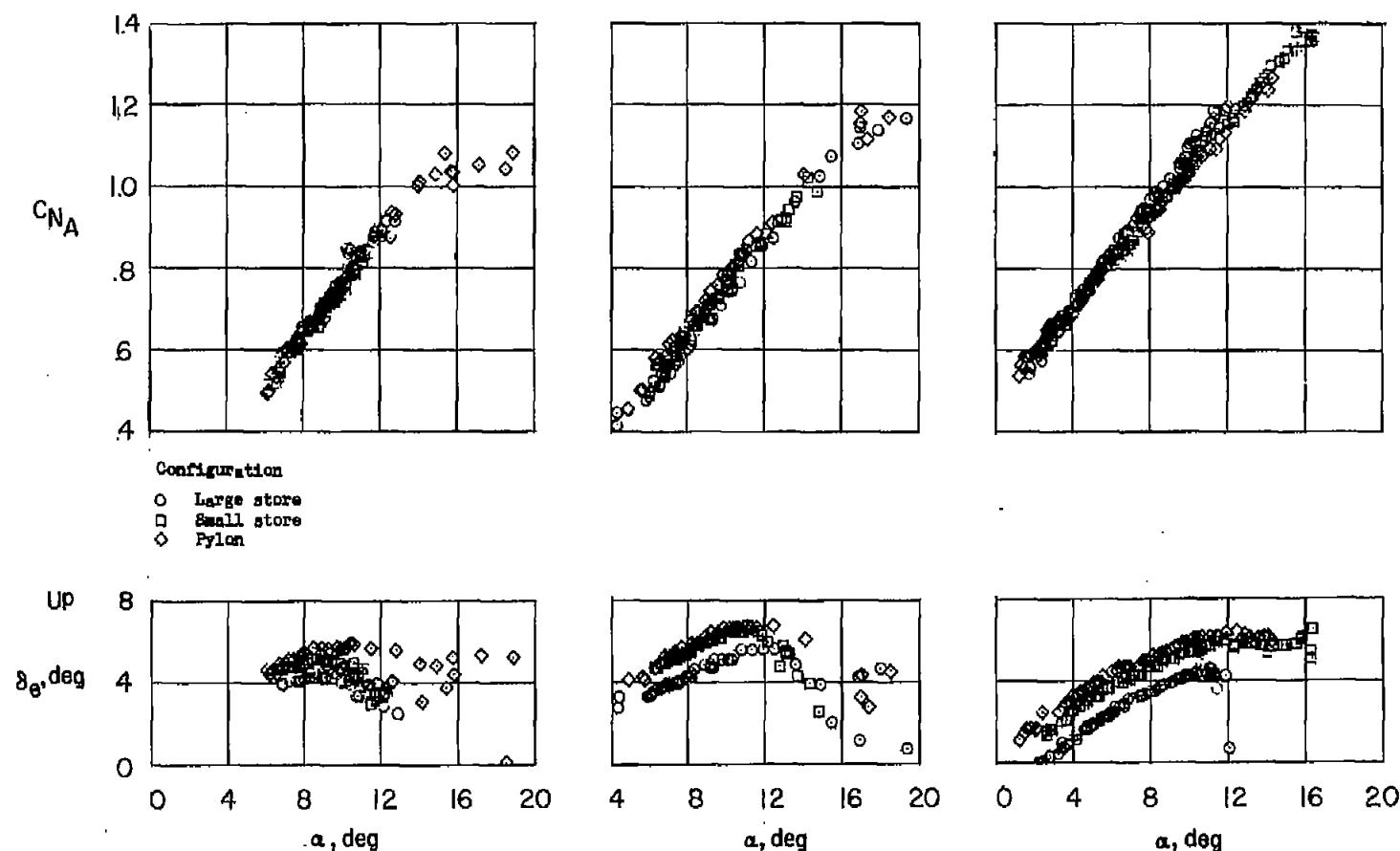
(b) Slats-unlocked condition.

Figure 13.- Continued.



(c) Landing condition.

Figure 13.- Concluded.



(a) Slats-locked condition. (b) Slats-unlocked condition. (c) Landing condition.

Figure 14.- Comparison of normal force and apparent stability characteristics obtained during stall approaches of the D-558-II airplane.

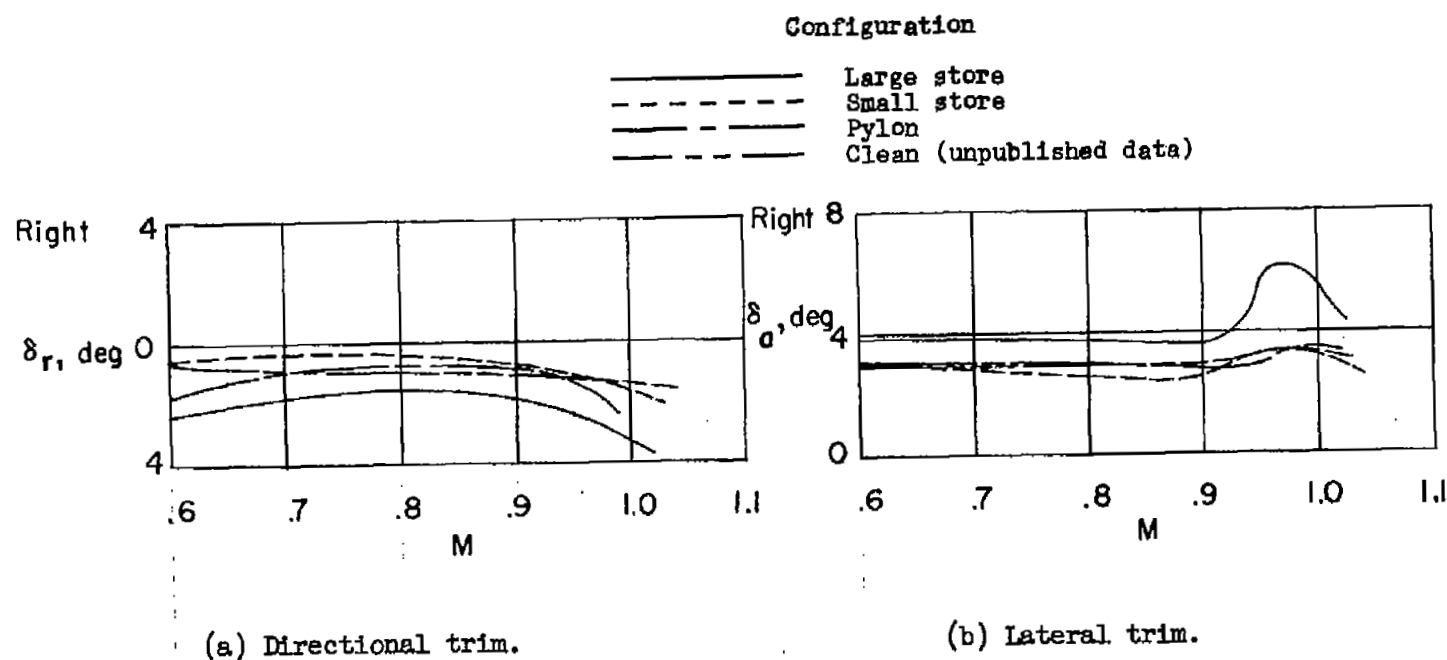


Figure 15.- Lateral and directional trim of the D-558-II airplane for the configurations tested.

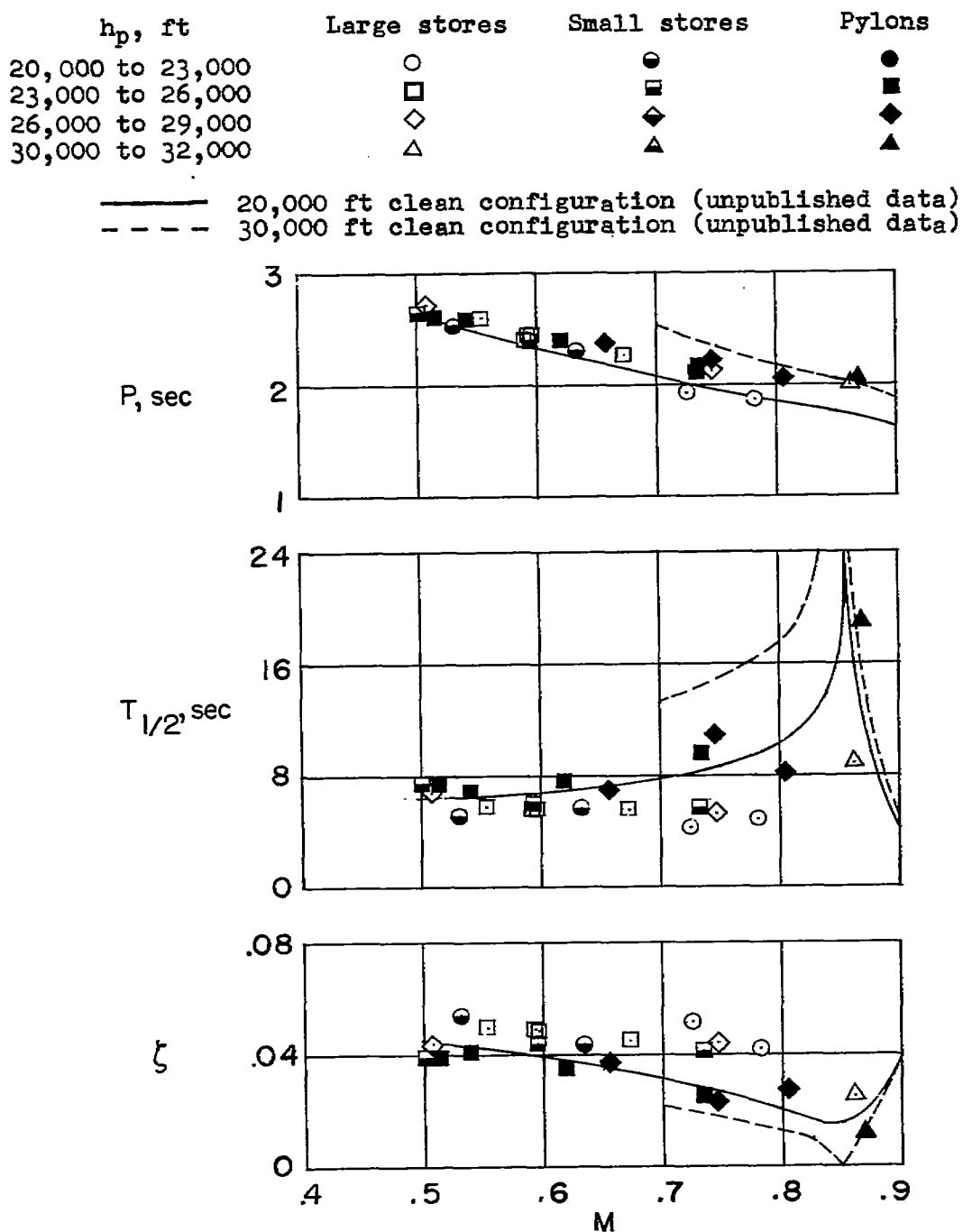
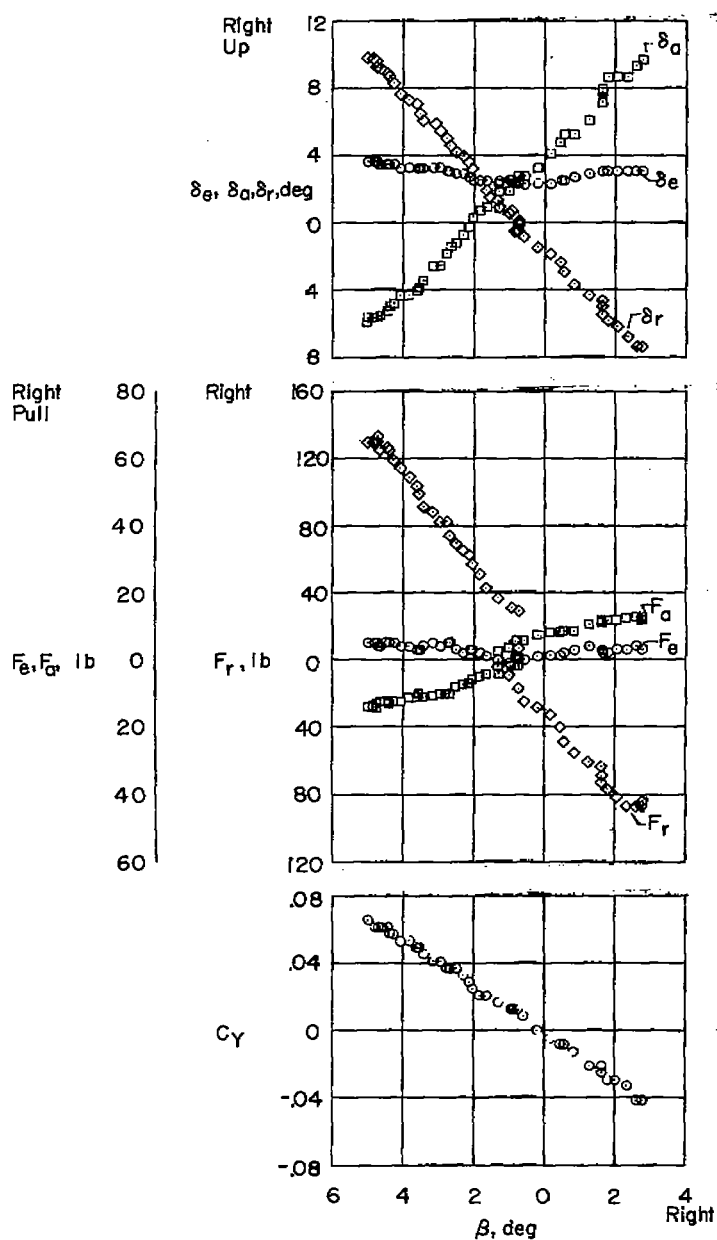
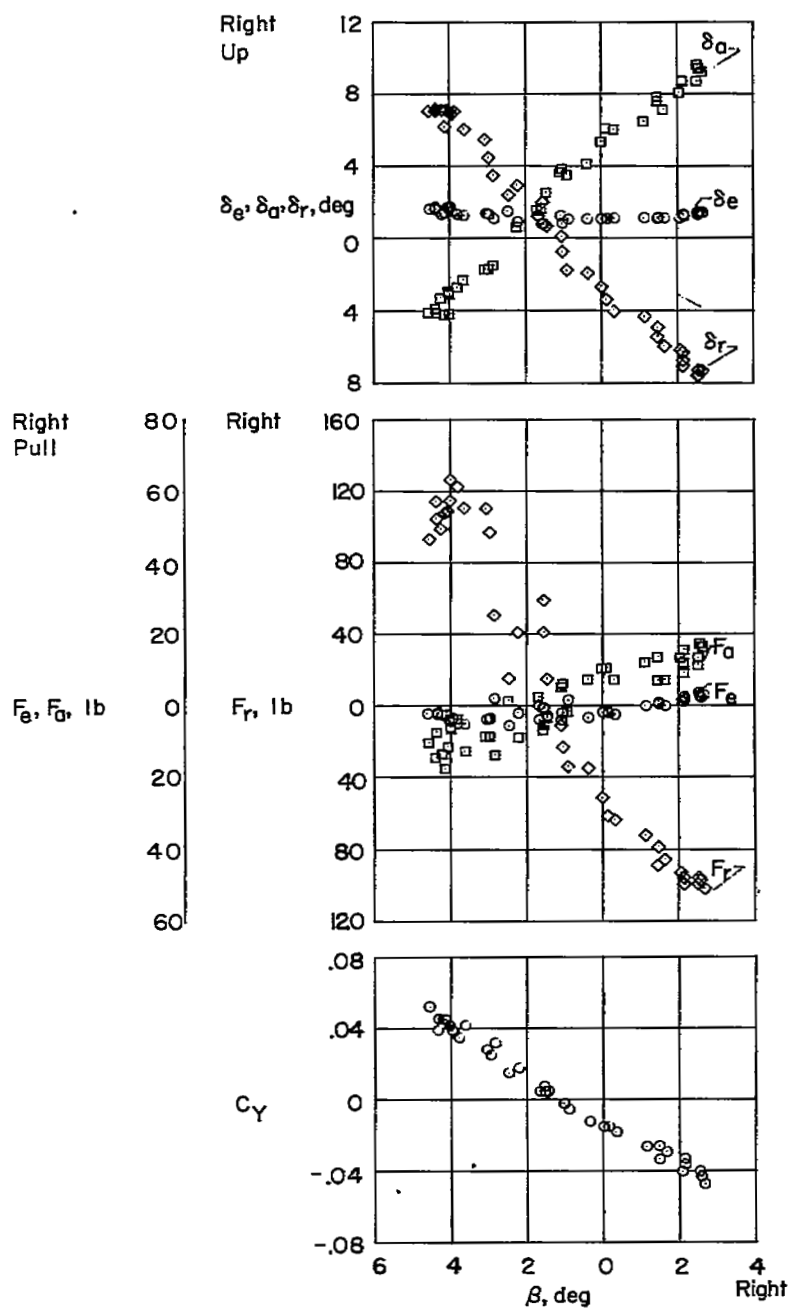


Figure 16.- Lateral dynamic characteristics of the D-558-II airplane for the configurations tested.



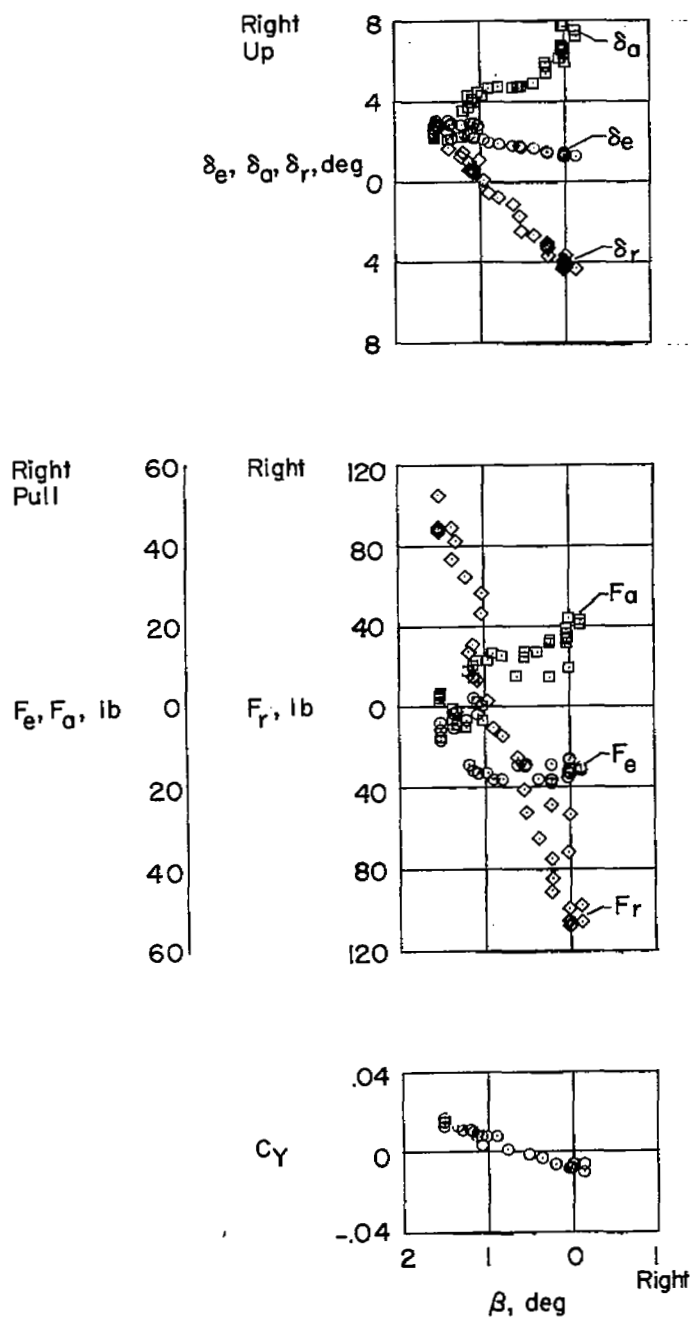
(a) $M \approx 0.55$; $h_p = 25,000$ feet.

Figure 17.- Typical variations of control positions, control forces, and side-force coefficient with sideslip angle for the D-558-II airplane, in the large-store configuration.



(b) $M \approx 0.80$; $h_p = 37,300$ feet.

Figure 17.- Continued.



(c) $M \approx 0.98$; $h_p \approx 36,000$ feet.

Figure 17.- Concluded.

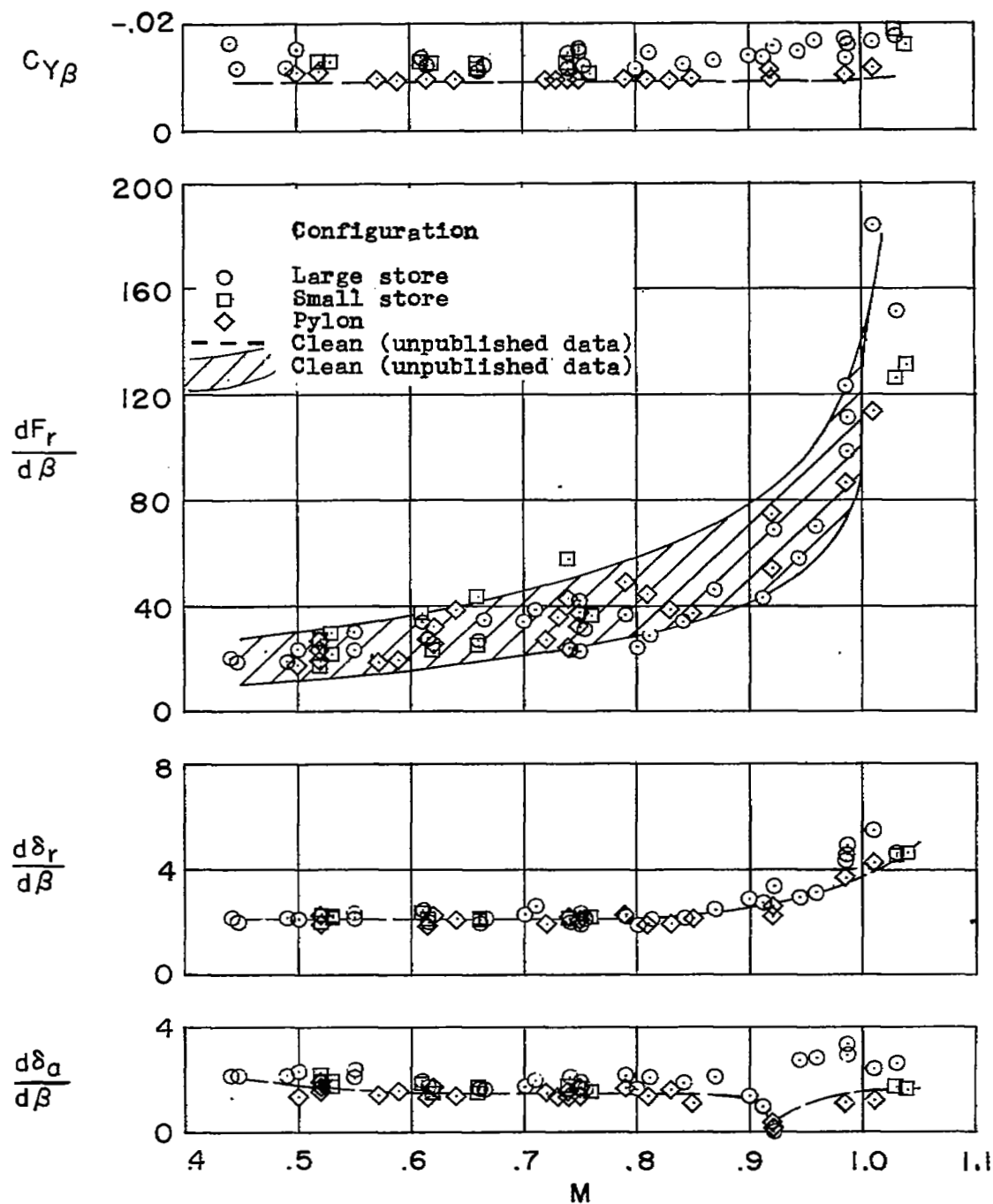


Figure 18.- Summary of the sideslip characteristics of the D-558-II airplane for the configurations tested.

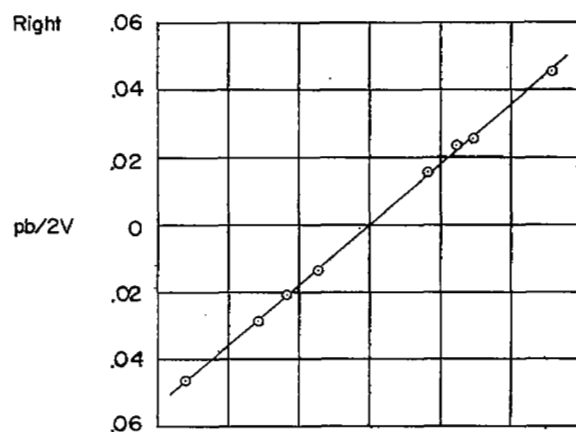
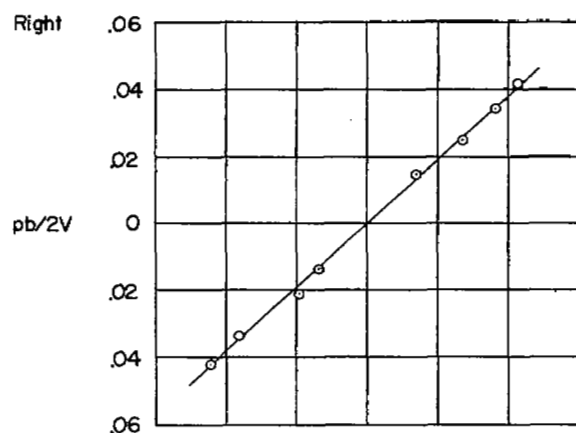
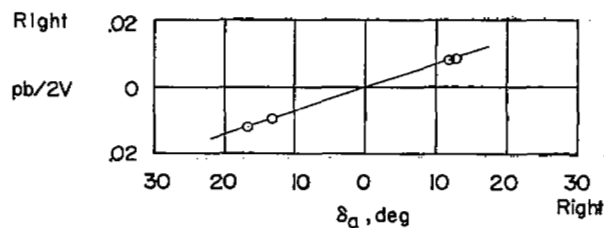
(a) $M = 0.48$ to 0.50 .(b) $M = 0.81$ to 0.84 .(c) $M = 0.98$ to 0.99 .

Figure 19.- Typical rolling characteristics of the D-558-II airplane in the large-store configuration.

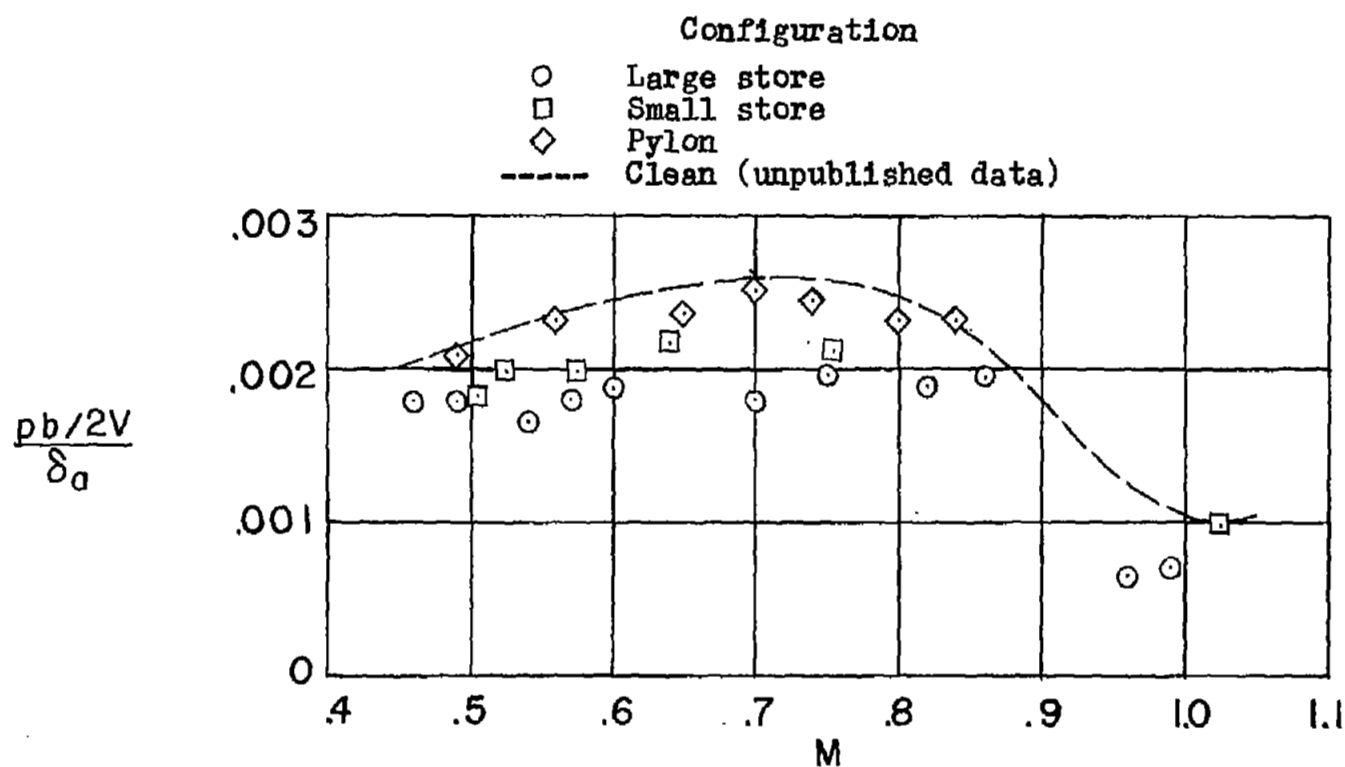



Figure 20.- Variation of $\frac{pb/2V}{\delta_a}$ with Mach number for the configurations tested,
D-558-II airplane.

[REDACTED]

NASA Technical Library



3 1176 01437 0036

[REDACTED]

[REDACTED]

[REDACTED]